26. RESULTS FROM STUDIES OF HIGHWAY GROOVING AND TEXTURING AT NASA WALLOPS STATION

By Walter B. Horne

NASA Langley Research Center

SUMMARY

Results of studies of the skid resistance obtained on 30 different pavement surfaces installed at the NASA Wallops Station airfield are discussed. Presented are transient peak, steady-state peak, and locked-wheel braking coefficients of friction for ASTM rib-tread and ASTM bald-tread tires and for new and worn production tires obtained under dry, wet, and flooded pavement conditions at vehicle speeds ranging from 10 to 80 mph. Results of limited vehicle spin-out tests on a 500-foot-radius highway curve are also included. It was found that the presently used method of making locked-wheel friction measurements to determine pavement skid resistance does not necessarily denote the true skid resistance of pavements under vehicle rolling or maneuvering conditions. Also, the skid resistance of smooth closed-texture pavements tends to be dangerously low under wet conditions when vehicles are operated at high speed with worn tires. However, the more open textured pavements as well as the transverse- and longitudinal-groove pavements exhibited adequate skid resistance for the vehicle speed and tire conditions investigated.

INTRODUCTION

Two factors which have always been present on the American highway scene in varying degree over the years have now reached a stage of growth to cause concern about future safety of the highway system. These factors are vehicle population frequenting the system and the speed which vehicles attain on highways.

The vehicle population using United States highways is growing rapidly and the Bureau of Public Roads estimates that 102 to 103 million vehicles will be in use during 1969. Since the end of World War II, the average speed of vehicles on our main highways has risen approximately 1 mile per hour per year.

The risk of accidents occurring on dry pavements during normal driving maneuvers is also increasing as the number of maneuvers increase due to the larger number of vehicles and the higher speeds involved. This becomes apparent when one notes that the tire-ground friction coefficient required to prevent vehicle spin-out while rounding curves or making lane changes increases as the square of the vehicle speed. The risk of accidents increases even more when pavements become wet or covered with slush, snow, and ice as a result of the reduction in available tire-ground friction coefficient. Limited

studies have shown that the average American motorist possesses driving habits which greatly influence highway safety. For example, he reduces his speed significantly under snow- and ice-covered pavement conditions. Thus, the motorist recognizes these hazardous driving conditions by reducing speed. On the other hand, the typical motorist tends to reduce speed only by 1 mile per hour when pavements are wet. Obviously he does not recognize that wet pavements can become equally hazardous under certain conditions. Many motorists also take pride in the number of miles their vehicles can obtain on a set of tires. Significant numbers of vehicles consequently are driven on the highway system with dangerously worn tires. Currently, many states are introducing or have introduced laws to eliminate this practice. Unfortunately, research shows that large differences in wet road grip still exist between a new tire and a tire worn to the legal wear limit, usually 1/16 inch of tread remaining.

With these considerations in mind, the Virginia Highway Research Council requested the assistance of the National Aeronautics and Space Administration in evaluating the skid resistance of different highway surface textures, coatings, and groove patterns under wet conditions at high speed. Several surfaces of each type mentioned were installed on the adjoining taxiway of the landing research runway at NASA Wallops Station in time for a limited evaluation by the highway vehicles and braking trailers participating in the Joint NASA-British Ministry of Technology Skid Correlation Study conducted during June 1968.

It is the purpose of the present paper to describe the changes in skid resistance which occur to these taxiway surfaces, as well as to the test surfaces on the landing research runway, as vehicle speeds increase from low values to as high as 80 miles per hour. This speed seems high by current highway standards, but trends indicate that this speed will be reached in the near future on the interstate highway system. The pavement surfaces were studied under dry, wet, and flooded conditions with ASTM rib- and bald-tread tires. Limited tests were conducted with new production tires and production tires worn to the legal wear limit. Most of the test data were obtained during vehicle braking although some cornering data were obtained on vehicles rounding a 500-foot-radius highway curve at speeds up to 50 miles per hour.

TEST SURFACES

The test surfaces investigated are located on three separate sites at the NASA Wallops Station airfield.

Site I

Site I is the landing research runway which is described in references 1 and 2. The surfaces installed on this runway were selected to cover the range of pavement textures presently in use on airport runways of this country. A short description and a photograph of each test surface on site I are presented in table I and figure 1, respectively.

Site II

Site II is the concrete taxiway of the landing research runway. The surfaces studied on this site were chosen on the basis of their applicability for use on highway pavements. Included in these test surfaces are several currently used highway groove patterns cut in both concrete and asphalt, sprayed and rolled epoxy overlays, a sand asphalt deslicking mix, and an asphalt overlay containing a synthetic aggregate. The layout of the site II test surfaces is shown in figure 2. A short description and a photograph of each test surface on site II are given in table II and figure 3, respectively. The groove patterns were cut into the pavement by using the diamond saw technique. It should be noted that the approaches to and the transitions between some of the site II test surfaces were at different elevations due to pavement overlays either used to seal coat the taxiway some years before the time of this study or installed immediately prior to the study to form test surfaces. The consequence was vehicle pitching or bouncing during the runs especially at the higher test speeds on some of the test surfaces. These vehicle oscillations during tests tended to increase the scatter of test data acquired on site II as compared with the scatter of test data acquired on the more level and uniform test surfaces of sites I and III.

Site III

Site III is a concrete hangar apron which was converted into a large rectangular skid pad as shown in figure 4. Yellow highway marking paint was used to outline both straight and curved traffic lanes on the skid pad. The approaches to the skid pad were such that cornering and braking tests performed on the skid pad had to be limited to a maximum vehicle speed of 50 miles per hour. A special feature of the skid pad was the installation of longitudinal highway grooves along a 500-foot-radius traffic lane. For comparison purposes, several concentric 500-foot-radius ungrooved traffic lanes were also installed on the skid pad (fig. 4). A short description and a photograph of each test surface on site III are presented in table III and figure 5, respectively.

Surface Conditions

It should be pointed out that none of the test surfaces of this study had been subjected to traffic, such as that experienced on highway pavements, before the start of testing. This point should be borne in mind when the test data are analyzed. For example, surface E of site II is an asphalt overlay containing a synthetic aggregate called Sinopal which is very white and purported to be highly skid resistant. The photograph of surface E taken at the conclusion of the tests (fig. 3) shows only a few white stones on the surface. In essence, the braking tests performed on this surface determined the skid resistance of the asphaltic binder adhering to the Sinopal aggregate rather than the skid

resistance of the Sinopal surface itself. If, however, this surface had experienced more traffic, much of the surface binder would have worn off; thus, a larger proportion of the Sinopal aggregate would be exposed and, as a result, different traction values would be obtained.

PAVEMENT WETTING TECHNIQUES

Site I

Three-thousand feet of pierced plastic pipe were placed along the edge of the runway test sections. The pipe was connected at 200-foot intervals with a water hydrant system located off the side of the runway. Through intermittent use of the sprinkler system a wet and puddled pavement condition was achieved on the desired test sections for test purposes. Continuous use of the sprinkler system produced a flooded condition on the test sections where the water depth was maintained at an average level of 0.1 inch on the pavement surfaces. Figure 6 illustrates the wet and puddled pavement condition achieved on surface A of site I during braking tests with the British "Juggernaut" test vehicle.

Several runs were made on surfaces A and C of site I under a slush cover. The slush was made by letting crushed ice melt on the runway surface until the desired slush level was reached. The test technique used is described in reference 2.

Site II

The plastic-pipe sprinkler system used on site I was also used on site II to wet the test surfaces. The flooded pavement condition is illustrated in figure 7(a) which shows the NASA diagonal braking car making a run on surface E of site II. The wet and puddled pavement condition used on site I was not used on site II. For the wet condition on site II, the sprinkler system was turned on to wet the pavement and then turned off. A powered rotary broom was then driven over the test surfaces to remove puddled water. This technique left the surface wet for test purposes but without water puddles. When the test surfaces were seen to be drying out, this procedure was repeated to maintain uniform test conditions.

Site III

The concrete apron forming the site III skid pad was a flat tilted slab. Pierced canvas fire hose was placed along the upper edge of the slab. When the sprinkler system was turned on, the water flowed from top to bottom which allowed a fairly uniform water film to be established over the entire skid pad surface. This sprinkler system is shown in operation to produce a flooded pavement condition in figure 7(b). The sprinkler system,

along with the powered rotary broom, was intermittently used to obtain a wet pavement condition without puddles for test purposes.

Vehicle spin-out tests were also conducted on the 500-foot-radius curves on the site III skid pad for an extremely slippery condition. This condition was obtained by the use of hydrolube or "instant banana peel." This material which is a white powder was sprinkled uniformly over the wet test surface. The powder immediately mixed with the water to form an extremely slippery film which bonded to the pavement surface. The test surface after a treatment of hydrolube was at least as slippery as wet smooth ice and as difficult to walk upon without slipping.

Test Tires

The tires used to determine the skid resistance of the test pavements are shown in figure 8. Most of the braking data described in this paper were obtained with ASTM bald-tread and rib-tread test tires which are described in reference 3. Limited braking data were obtained with a typical production tire worn to the point that the wear markers of the tread were showing. Highway safety laws currently in effect in some states require that tires be replaced when this stage of wear is reached.

The ASTM bald-tread tire, the worn production tire, and a new production tire of the same tread design as the worn tire were used in unbraked vehicle spin-out tests on site III to determine the skid resistance of curved pavement.

Test Vehicles

It is beyond the scope of this paper to present all the braking data obtained by the different test vehicles that participated in the Joint NASA-British Ministry of Technology Skid Correlation Study. Instead, selected braking data obtained with the General Motors braking trailer, the FAA Swedish Skiddometer, the B. F. Goodrich diagonal braking car, and the NASA diagonal braking car are presented for pavement skid resistance comparisons. Most of the data presented were obtained during the Joint Correlation Study although some data with the NASA diagonal braking car were obtained after the conclusion of the correlation study. These data include, for example, the braking results obtained on site II test surfaces under flooded pavement conditions. The vehicle spin-out tests on site III were also conducted after the conclusion of the skid correlation study. Participating vehicles for this study were the B. F. Goodrich diagonal braking car and a stripped convertible with protective cage operated by NASA.

The operating characteristics of the General Motors braking trailer, FAA Swedish Skiddometer, B. F. Goodrich diagonal braking car, and the NASA diagonal braking car are described in reference 3. The NASA stripped convertible used in the vehicle spin-out tests on site III is shown in figure 9.

SKID RESISTANCE OF TEST SURFACES

Braking and cornering friction data obtained under dry, wet, and flooded conditions on the 30 surfaces of sites I, II, and III are discussed in this section. Also included are braking data on several surfaces of site I under slush-covered and ice-covered pavement conditions. Some vehicle spin-out or cornering data obtained on the 500-foot-radius grooved and ungrooved highway curve test surfaces of site III under an extremely slippery pavement condition effected by using hydrolube and water are also presented.

The maximum skid resistance of a pavement normally occurs under dry conditions. A considerable effort, and quite a few test tires, was expended to obtain dry-surface braking data on all the test surfaces so that a firm base could be established to rate the relative skid resistance of the test surfaces under wet conditions.

Site I Surfaces

Dry conditions.- The dry-surface skid resistance of site I surfaces was rated by the NASA diagonal braking car. A Tapley meter installed in this car measured an effective friction coefficient μ_{eff} which is between transient peak μ_{max} and locked-wheel μ_{skid} friction-coefficient values. These data are presented in figure 10 where effective friction coefficient μ_{eff} is plotted as a function of ground speed. It is interesting to note that no significant differences in dry-surface friction values exist between the ungrooved or grooved surfaces of site I at speeds up to 60 miles per hour. The data in figure 10 indicate that the dry-surface friction values for the ASTM rib-tread tire are somewhat lower than those for the ASTM bald-tread tire, especially at medium test speeds.

A similar presentation of dry-surface braking results for the FAA Swedish Skiddometer on site I surfaces is given in figure 11. It should be noted that the Swedish Skiddometer measures the maximum steady-state braking friction coefficient that occurs at a slip ratio of 0.13. The Skiddometer used the ASTM bald-tread tire for this evaluation. Again, the dry-surface skid-resistance values of the ungrooved surfaces are close together and the grooved surface values are also close together over the speed range from 10 to 80 miles per hour covered in these tests. The peak friction coefficients μ_{max}, however, measured by the Skiddometer indicate slightly higher dry-surface friction values for the grooved surfaces than for the ungrooved surfaces of site I. This is an interesting result in that the 1- × 1/4- × 1/4-inch groove pattern used in site I actually removes 25 percent of the pavement surface and thereby increases the tire-ground bearing pressure by 25 percent. Aeronautical tire research has shown that the dry-surface friction coefficient developed by tires on pavements decreases with increasing bearing pressure between tire and ground (ref. 4). The Skiddometer results as well as

the diagonal braking car results infer that tire-groove interlocking effects may account for this benefit.

Wet and puddled conditions.- The skid resistance of site I surfaces for a wet and puddled runway condition was rated with the NASA diagonal braking car and the data are presented in figure 12. Values of μ_{skid} were obtained in this case from a recording accelerometer installed in the car, and these measurements were made during the time that the wheels were in a locked-wheel skid condition. In the figure, μ_{skid} values obtained for the ASTM bald-tread tire and the ASTM rib-tread tire are plotted as a function of ground speed. On the ungrooved pavements, the best surface for the bald-tread tire at 40 miles per hour is surface E (Gripstop), a sand-type asphalt. At a speed of 70 miles per hour this surface is among the worst. At 70 miles per hour, not one of the ungrooved surfaces of site I provides adequate traction for a bald-tread tire in a locked-wheel condition. The results for the ASTM rib-tread tire show much better pavement skid resistance. At 40 miles per hour, all ungrooved surfaces of site I show a μ_{skid} value of 0.37 or better. The value of 0.37 has been proposed as a minimum skid standard for pavements by Kummer and Meyer in reference 5. It is noticed in the figure that at 70 miles per hour all μ_{skid} values of the ungrooved surfaces fall below this value. Placing 1- × 1/4- × 1/4-inch transverse grooves in the pavements raises the skid resistance of site I surfaces so that at 70 miles per hour the skid values for ASTM bald- and rib-tread tires meet this standard on all surfaces with the exception of surface B which has a value of 0.35 for the bald-tread tire.

The FAA Swedish Skiddometer, using a self-watering system, was also employed to rate the relative skid resistance of site I surfaces. The results obtained with the ASTM bald-tread tire are shown in the lower graphs of figure 11. The self-watering technique deposited a continuous water film 0.02 inch thick on the dry pavement immediately ahead of the test tire.

For the ungrooved surfaces, the surfaces having the least skid resistance at 80 miles per hour were surfaces A and E which were canvas belt concrete and Gripstop. The best surface was surface I, the plant mix asphalt with 3/4-inch aggregate. These results tend to conform with NASA grease test measurements of average pavement texture depth made on the surfaces of site I, as shown in the following table:

Site I surface	NASA grease test average texture depth, mm	FAA Skiddometer steady-state braking friction coefficient at 80 mph, μ_{max}
A . . .	0.12	0.19
D . . .	0.20	0.3
E . . .	0.14	0.19
F . . .	0.19	0.23
I . . .	0.32	0.4

The surfaces having the best skid resistance also had the largest average pavement texture depth. These results indicate that for high-speed operations, a pavement should have an open texture to provide external water drainage between tire and ground.

The remarkable effectiveness of 1- × 1/4- × 1/4-inch transverse pavement grooves in improving wet pavement skid resistance is also shown in figure 11. At 80 miles per hour, the wet peak braking values are only slightly lower than the dry values. In fact, over most of the speed range, the wet values are higher than the dry values. This result is attributed to a water cooling effect since the ASTM bald tire tread rubber was found to be extremely hot to the touch when running at peak braking conditions on dry pavements. It should be noted in figure 11 that the transverse-groove pattern on site I restores the wet-surface skid resistance of a bald-tread tire to dry-surface values while rolling under peak braking conditions. Grooving is not as effective on wet pavements when the tire operates in a locked-wheel braking mode. The data in figure 12 indicate that the μ_{skid} values obtained on wet grooved pavements are significantly less than the dry-surface friction values although they are substantially higher than the μ_{skid} values obtained on wet ungrooved pavements at high speed.

The effect of increasing pavement texture depth on pavement skid resistance is shown in figure 13. In this figure μ_{eff} values obtained on concrete surfaces A and B of site I which have a canvas belt drag surface treatment are compared with μ_{eff} values obtained on surfaces A-1 and B-1 which actually are surfaces A and B given a spray coating of epoxy-grit. The average grit size is 3/32 inch. The void areas between the grit particles on the pavement surface provided more external water drainage capacity and improved the skid resistance of both grooved and ungrooved pavements even when a worn tire was used on the test vehicle under flooded pavement conditions.

A most important feature of the pavement grooving used on site I is the restoration of the skid resistance of worn tires on wet pavements to resistance values of new tires. This feature was first noted during the aircraft tests on site I. Figure 12 illustrates this point with ASTM bald- and rib-tread tires. The B. F. Goodrich diagonal braking car also made braking tests with a worn production tire and the ASTM rib-tread tire under flooded pavement conditions on surfaces C and D of site I. These results are compared in figure 14. It can be seen that the worn tire (wear markers showing) at speeds greater than 40 miles per hour on the ungrooved concrete has less than one-half the skid resistance of the ASTM rib-tread tire, yet on the 1- × 1/4- × 1/4-inch transverse-groove pavement both tires have about equal skid resistance.

Slush conditions.- Several tests were made on surfaces A (ungrooved) and C (grooved) of site I where a slush layer ranging from 0.5 to 2 inches covered the pavement. This slush layer quickly became rutted with the passage of vehicles during tests. Figure 15 presents the skid resistance of these pavements under this slush cover in terms

of transient peak μ_{max} (ref. 3) and locked-wheel μ_{skid} friction coefficients for both ASTM bald- and rib-tread tires. It can be seen that the ASTM rib-tread tire develops higher friction coefficients than the ASTM bald-tread tire on ungrooved surface A. It is also of interest to note that no significant difference exists between the ASTM rib-tread-tire transient peak μ_{max} and locked-wheel μ_{skid} friction coefficients at 60 miles per hour on the ungrooved surface. This result indicates that some, if not all, of the apparent friction coefficient developed at this speed may be due to slush displacement drag acting on the tire rather than from adhesion forces acting between tire and ground. The friction coefficients for grooved surface C are higher than those for ungrooved surface A at speeds below 60 miles per hour.

Ice conditions.- An icy runway condition developed during testing of the F-4D aircraft on site I. From results of automobile tests presented in table IV, considerable improvement in pavement skid resistance was noted for the grooved pavement over the ungrooved pavement. In fact, during tests where braking was initiated at 50 miles per hour, the average friction coefficient on the grooved surface became nearly double that on the ungrooved surface. Similar improvement in skid resistance on ice was noted during steering tests with another car employing half-worn tires (fig. 16). It should be noted that for this temperature of 31° F, the ice was thin and not firmly bonded to the pavement surface. Another test was made with water sprayed through a fog nozzle on surfaces F and G of site I at an ambient temperature of 18° F. At this temperature, the thin coating of ice that formed on the surface developed a hard bond with the pavement. Locked-wheel tests with the NASA diagonal braking car and ASTM bald-tread tires showed much less skid resistance for both the grooved and ungrooved surfaces for this condition as compared with the results at 31° F. In fact, at 50 miles per hour, the car only developed a μ_{skid} value of 0.08 on grooved surface G and a μ_{skid} value of 0.04 on ungrooved surface F. From these results, it is apparent that pavement grooving improves pavement skid resistance under icy conditions but is of practical benefit in braking vehicles only near temperatures when ice is first formed, that is, near 32° F. Steering tests were not made for the cold icy condition (18° F) and, therefore, the benefit from grooving is not known for this vehicle operating condition.

Site II Surfaces

Dry conditions.- The NASA diagonal braking car equipped with ASTM bald-tread tires and using a Tapley meter to measure vehicle braking was employed to rate the dry-surface skid resistance of the 13 pavement surfaces of site II. The effective friction coefficient is presented as a function of vehicle ground speed for the site II surfaces in figures 17 to 21. Although the scatter of data for the site II surfaces is considerably more than that for the site I surfaces in figure 10, the average values obtained on site II surfaces

are in agreement with site I dry-surface friction-coefficient values. As previously mentioned in the section entitled "Test Surfaces," this increase in test-data scatter for site II surfaces is attributed to vehicle pitching and bouncing caused by the more uneven test surfaces of site II.

Wet conditions.- Unfortunately, a poor choice was made on the wetness condition for site II surfaces during the Joint Correlation Study. As was described in the section entitled "Pavement Wetting Techniques," a powered rotary broom was used to remove all puddled water from the test surfaces. This wetness condition was insufficient to create major changes in skid resistance between the different test surfaces, especially if ASTM rib-tread tires were used on the test vehicles. This wetness condition, although classified as wet, was in reality a damp surface such as that which might occur on a highway after a rain had stopped falling and vehicular traffic had removed any puddled water from the pavement.

After the completion of the Joint Correlation Study, the NASA diagonal braking car was rerun over the site II surfaces under a flooded pavement condition described in the section entitled "Pavement Wetting Techniques." ASTM bald-tread tires were used and the Tapley meter was employed to measure vehicle braking. As previously discussed, this vehicle braking technique and measuring system creates an effective friction coefficient which lies between the transient peak μ_{max} and locked-wheel μ_{skid} friction values.

Figure 17 shows the skid-resistance rating by the NASA diagonal braking car of the more conventional test surfaces of site II under the aforementioned dry, wet, and flooded conditions. It can be seen that the skid resistance for all surfaces in figure 17 decreased from dry-surface values as speed increased for this essentially damp pavement condition. Larger losses in skid resistance developed on the surfaces under flooded pavement conditions. All surfaces in figure 17 had a closed texture with a small average texture depth (fig. 3). These results are in agreement with results obtained on site I surfaces which showed the smooth closed-texture-pavement surfaces as having poor skid resistance at high speed under wet conditions.

The improved skid resistance that more open-texture-pavement surfaces provide under wet and flooded conditions is illustrated in figure 18. This figure compares the skid resistance of surfaces C, E, F, and G which, as indicated in figure 3, had higher average texture depths than surfaces A, B, and D. The order of improvement in skid resistance for the surfaces shown in figure 18 apparently follows the degree of texturing provided in the surface.

Figure 19 shows the improvement in skid resistance gained when the 25-year-old concrete surface A of site II is provided with 3/4- × 1/8- × 1/8-inch transverse or longitudinal grooves. This groove pattern is typical of that being used in current highway

grooving. Both the transverse and longitudinal groove patterns used improved the pavement skid resistance under the wet and flooded test conditions as is noted by the higher and therefore safer friction values. The transverse-groove pattern also restored more of the dry-surface skid performance of the pavement than did the longitudinal-groove pattern. The improvement in skid resistance for the best groove pattern was about equal to that obtained by the asphalt dressing treatment shown in figure 18 for flooded pavement conditions. Similar results are shown in figure 20 where surface B, the 13-year-old asphalt seal coat of site II, was provided with the same 3/4- × 1/8- × 1/8-inch transverse and longitudinal grooves as the 25-year-old concrete surface A. An interesting result shown in figure 20 for the flooded pavement condition is that the longitudinal-groove pattern is as effective at 70 miles per hour as the transverse-groove pattern in raising the surface skid resistance.

Figure 21 shows the improvement in skid resistance obtained on surface B, the 13-year-old asphalt seal coat, when 1- × 1/8- × 1/8-inch transverse- and longitudinal-groove patterns were cut in the surface. Comparison of these data with the 3/4-inch-groove data presented in figure 20 reveals that the 1-inch grooves (fig. 21) are as effective as the 3/4-inch grooves when the surface is wet. Under flooded conditions, the 3/4-inch groove pattern with its higher water-drainage capacity provides the greater improvement in skid resistance to surface B.

Site III Surfaces

Dry conditions.- Figure 22 presents effective dry-surface friction coefficients measured by the NASA diagonal braking car on the specially prepared skid pad of site III. The skid pad was covered with a liquid coating of Jennite, a coal-tar product, without the sand or aggregate content that is normally used when Jennite is applied to highway surfaces. (See table III.)

It is important to note that the ASTM bald-tread-tire dry-surface friction values obtained on site III surfaces are somewhat less than those obtained on site I surfaces. (Compare figs. 22 and 10.) On the other hand, larger differences in dry-surface friction values exist between site I and site III surfaces for the ASTM rib-tread tire. The reason for the low ASTM rib-tread-tire dry-surface friction values on site III surfaces is not known at the present time.

Wet and flooded conditions.- The NASA convertible test car shown in figure 9 was equipped with a Tapley meter mounted on the floor of the car and sideways to the direction of vehicle motion. The test car was then driven at increasing speeds around the 500-foot-radius grooved and ungrooved curves of site III until vehicle spin-out occurred. The lateral friction coefficients and spin-out speeds obtained with the test vehicle equipped with ASTM bald-tread tires, new production tires, and worn production tires (wear marker

showing) are shown in figure 23(a) for a wet pavement condition (surface wet but no puddles). Photographs of these tires are shown in figure 8. The wet pavement condition was achieved by driving a powered rotary broom over the test surface to remove surplus water from the surface after it was initially wetted by the sprinkler system installed at site III. The data shown indicate that longitudinal grooves on a highway curve can improve the skid resistance of a pavement when ASTM bald-tread and worn production tires are used on a vehicle. The maximum test speed for site III of 50 miles per hour was obtained before spin-out conditions occurred for the new production tire tested. This result shows the importance of having and maintaining an effective tread design on road vehicle tires.

The same tire tread configurations were tested on the NASA convertible under flooded pavement conditions and the results are shown in figure 23(b). For the flooded ungrooved curve, all tires regardless of tread design caused the vehicle to spin-out at about 38 miles per hour. The vehicle spin-out speed and skid resistance of the pavement were improved by grooving the highway curve, as also shown in figure 23(b).

Many different opinions have been expressed to explain the improved performance of vehicles operating on grooved wet or flooded pavements as contrasted with vehicle performance obtained under similar conditions on ungrooved pavements. Among these are better water drainage through the low-pressure escape channels provided by grooving and the biting of the sharp edges of groove corners into the tire and displacing the viscous and tenacious fluid film which separates tire from pavement. Also, it has been suggested that the tire tread rubber penetrates into the pavement grooves under operating conditions and it is this interlocking or gear effect plus possibly the groove edge effect which produces the improvement in skid resistance. In an attempt to isolate this interlocking effect, the following experiment was performed. Hydrolube or "instant banana peel" was mixed with water on the test surfaces of site III. This technique produced a slippery pavement condition, at least as slippery as wet ice. It was hoped that such a slippery condition would reduce tire-ground adhesion to minimal values so that any improvement in skid resistance on the grooved pavement must come from the interlocking effect. The results of the experiment are shown in figure 24. On the lubricated ungrooved pavement, the spin-out speeds for the two test vehicles, a sedan and a convertible, were extremely close but very low. In fact, the spin-out speed was only 15 miles per hour regardless of whether a new production tire or an ASTM bald-tread tire was used. The test results on the lubricated grooved surfaces showed a large improvement in skid resistance from longitudinal grooving for both tire designs. These results tend to confirm the presence of a mechanical interlocking effect between a tire and grooved pavement. Further corroboration of the interlocking effect is evident by the audible rumble produced by the tires when the test vehicle starts to slide sideways on a longitudinally grooved pavement. The sideways-mounted recording accelerometer placed in the B. F. Goodrich test car also showed a ripple in its acceleration trace when the car slid sideways on the grooved pavement.

The results from highway grooving in California have provided the researcher a most exasperating paradox. On every highway where grooves were installed, vehicle accident rates under wet pavement conditions fell dramatically. Yet skid resistance tests before and after grooving showed very little difference in friction coefficient, hardly enough to account for the dramatic accident rate reduction due to grooving. Grooving tests have been made by other states with basically similar unrewarding skid resistance results. The vehicle spin-out tests along with vehicle braking tests made on site III have furnished sufficient data to explain this paradox. In figure 22 are presented the vehicle spin-out lateral friction coefficients obtained with the NASA convertible car (fig. 23(b)) and near transient peak braking friction coefficients obtained with the NASA diagonal braking car using a Tapley meter under flooded conditions. It can be seen that, although the agreement between lateral and braking measurements is fair, the braking values are lower than the actual lateral friction-coefficient values occurring at spin-out on the curve. Figure 25 presents transient peak μ_{max} and locked-wheel μ_{skid} friction-coefficient data obtained with the General Motors braking trailer on the grooved and ungrooved curves of the site III skid pad for ASTM bald- and rib-tread tires. Also shown are the lateral friction coefficients obtained at spin-out speeds occurring to the NASA convertible test car (fig. 23(b)) when equipped with ASTM bald- and rib-tread tires. Finally, the steady-state peak μ_{max} braking coefficients obtained with the FAA Swedish Skiddometer equipped with ASTM bald-tread tires are shown.

It first should be pointed out that the μ_{skid} values obtained by the General Motors braking trailer (fig. 25) indicate little improvement in skid resistance between grooved and ungrooved pavement surfaces for either ASTM rib- or bald-tread tires. This result is consistent with the experience of California and other states when testing grooved pavements with braking trailers. On the other hand, the actual vehicle spin-out data on the curves in figures 23, 24, and 25 show an improvement in skid resistance between grooved and ungrooved pavements. It is interesting to note that the transient peak braking coefficients by the General Motors braking trailer show a large improvement in skid resistance when the pavement is grooved. These data are corroborated by the FAA Skiddometer, the steady-state peak braking friction data of which show a similar improvement in skid resistance for the grooved surface. The General Motors data also show that pavement grooving raises ASTM bald-tread-tire peak friction levels to the level attained by the ASTM rib-tread tire.

The NASA research truck, which has the capability of measuring transient peak and locked-wheel braking coefficients of friction as well as steady-state peak lateral coefficient of friction, participated in the Florida Skid Correlation Study. Figure 26 presents some of the data obtained on five of the test surfaces under a wet pavement condition with the ASTM rib-tread tire and a production radial-tread tire. It can be seen that the transient peak braking coefficient was in close agreement with the steady-state peak lateral

coefficient of friction. Also, the locked-wheel friction coefficient was considerably less than either peak values, especially on the lowest skid resistance surface (painted concrete).

With these results in mind, it is fairly obvious that when a vehicle spins out on a highway curve or while making a lane change, it must first pass through the incipient skid point of the lateral-force-slip curve. This means that the steady-state peak lateral friction determines the skid resistance of the pavement for this vehicle operating condition. Since the data in figure 26 indicate that transient peak braking measurements are in close agreement with steady-state lateral-friction values, the transient peak braking coefficient may be used for this purpose as well.

Therefore, the skid resistance of a pavement for vehicles undergoing spin-out on highway curves or suffering loss of directional control from other tire cornering deficiencies is determined by incipient skid tire conditions which may be obtained from either steady-state peak lateral or transient peak or steady-state peak braking coefficients of friction. The skid resistance of a pavement for this vehicle operating condition cannot be obtained by locked-wheel skid-friction-coefficient measurements.

Another point can be gained from the data presented in figure 25. It will be noticed that spin-out values of lateral friction coefficient tend to be lower than the transient peak braking values. This fact is attributed to the method of test. For example, the test drivers were told to maintain constant speed through the curve during the spin-out tests by use of throttle. Thus, the rear driving tires of the vehicles had to develop a forward tractive force as well as a lateral force on the curve. It is believed that this factor, and perhaps vehicle suspension effects as well, account for the difference in results.

CONCLUDING REMARKS

Test results have been presented of the skid resistance obtained on 30 different pavement surfaces installed at the NASA Wallops Station airfield. The skid resistance of these pavements was determined by the use of ASTM rib- and bald-tread tires and by new and worn production tires mounted on test vehicles which measured transient peak, steady-state peak, and locked-wheel braking coefficients of friction. Limited vehicle spin-out tests on a 500-foot-radius highway curve were also made to study the skid resistance of pavements under this vehicle operating condition.

On the basis of results of the present highway grooving and texturing studies, some suggestions are included for improving the techniques for measuring skid resistance and for improving the skid resistance of pavements.

Improving the Techniques for Measuring Pavement Skid Resistance

At the present time, some highway agencies employ braking trailers which make locked-wheel skid tests on ASTM rib-tread tires to study pavement skid resistance. Unfortunately, such equipment supplies only a small part of the information required to depict the true skid resistance of a pavement. For example, the typical automobile spends most of its operating hours under rolling conditions on highways and very few hours undergoing panic stop situations where the wheels are inadvertently locked. The data in this paper show extremely large differences in tire traction performance for all pavements and wetness conditions depending upon whether the vehicle-tire operating mode is rolling under transient braking peak, or rolling at steady-state lateral or cornering peak, or undergoing a locked-wheel braking skid. It has also been demonstrated herein that the locked-wheel friction coefficient μ_{skid} considerably underestimates the ability of grooved pavements to improve pavement skid resistance on freeways or the open road under wet conditions.

For the open road driving or maneuvering condition, a vehicle before it skids must first pass through the peak or maximum point of the friction-coefficient slip-ratio curve. Thus, it is the peak friction coefficient rather than the locked-wheel friction coefficient μ_{skid} that depicts the true skid resistance of the pavement for this driving situation. For highway or street intersections where heavy vehicle braking is employed, more consideration should be given to the locked-wheel friction coefficient μ_{skid} rather than to peak friction coefficient in assessing pavement skid resistance for this driving situation. It follows from this discussion that pavement skid resistance measuring equipment must measure peak as well as skidding coefficients of friction to properly assess pavement skid resistance.

If all vehicles using the highway system of this country could be surveyed at one point in time, this survey should show that 25 percent of the vehicles have new tires, 25 percent have bald-tread tires or tires with the wear markers showing, and 50 percent have tires with wear between these two extremes. The results of the present study show that the skid resistance for open-texture and grooved pavement surfaces is insensitive to tire wear, whereas for most other pavement surfaces skid resistance is extremely sensitive to tire wear especially when tires are worn to the point of replacement. It follows therefore that pavement skid resistance measurements should be made on the ASTM bald-tread tire as well as the ASTM rib-tread tire to establish upper and lower bounds of skid resistance values to account for tire wear effects.

The fortunate correlation of steady-state or transient peak braking coefficients with steady-state lateral or cornering peak coefficient of friction shown in this paper means that these peak braking coefficients can be used to determine the lateral skid resistance of a pavement. From the foregoing considerations, it is suggested that second-generation

braking trailers be of the two-wheel braking type with an ASTM bald-tread tire on one wheel and an ASTM rib-tread tire on the other wheel. The measuring equipment of the trailer should be capable of measuring both transient peak and locked-wheel braking coefficients for both wheels. The friction-coefficient values obtained during test establish the upper and lower bounds of pavement skid resistance for vehicle directional control and braking modes of operation, respectively, as well as upper and lower bounds for new and worn tire effects. With this information, the highway engineer can consider the pavement – street intersection or open highway – and more accurately determine whether the pavement is safe for continued operation or should be treated before further use. It is also suggested that the second-generation braking trailer and towing vehicle have high-speed testing capability so that the skid resistance of high speed highways can be determined for actual vehicle operating speed conditions.

Improving Pavement Skid Resistance

The present study shows that the skid resistance of most of the pavement surfaces investigated can safely support vehicle operations as high as 80 miles per hour under wet conditions as long as the ASTM rib-tread tire or the production equivalent tire is used on the vehicle. On the other hand, when worn tires or ASTM bald-tread tires are used on vehicles, the skid resistance of the low average texture depth pavements, such as the sand asphalt and canvas belt concrete surfaces, drops to marginal values at this speed. This situation becomes worse as the water-film thickness on the pavement increases. It has been shown in this paper that open-texture pavements provide much better skid resistance than closed-texture pavements at speeds of 70 miles per hour even under flooded conditions. It follows, then, that high speed highways should be provided with a deeper, more open textured surface than is ordinarily used on highways with low speed limits, such as city streets. Highway engineers point out that open-texture pavements polish more than closed-texture pavements under heavy traffic conditions and, therefore, such surface treatment could create a greater pavement slipperiness problem at a future time. The answer to this polishing problem must be in the selection of minimum polishing aggregate for use in the wearing course of such pavements. If such local natural aggregate is not available, consideration should be given to the use of the new synthetic aggregates that are now coming into production and that possess the desired skid and polish resistant properties.

A most promising approach to improve pavement skid resistance is by pavement grooving. Transverse and longitudinal grooving of crowned pavements significantly increases the drainage of water from a pavement during times of precipitation. Consequently, the water-film thickness on the tire-pavement interface is reduced.

Both longitudinal and transverse highway grooves and the larger runway grooves studied demonstrated repeatedly the capability of not only improving new tire performance on wet or flooded pavements but also restoring worn and bald-tread-tire friction levels to new tire performance levels. Thus, grooved pavements tend to have only one set of pavement skid resistance boundaries: one upper boundary for the peak braking or cornering tire operating mode and one lower boundary for the locked-wheel skid tire operating mode. With the exception of very open textured pavements, most other pavement textures have two sets of boundary values for pavement skid resistance to account for tire wear effects.

Pavement skid resistance can be dramatically improved by eliminating the lower boundary due to locked-wheel vehicle operation. This can be accomplished by the mandatory use of antiskid braking systems on ground vehicles when such systems are perfected.

REFERENCES

1. Allen, Curtis R.; and Quillen, James W.: Problem Areas Associated With the Construction and Operation of the Landing Research Runway at NASA Wallops Station. Pavement Grooving and Traction Studies, NASA SP-5073, 1969. (Paper No. 8 herein.)

2. Yager, Thomas J.: Comparative Braking Performance of Various Aircraft on Grooved and Ungrooved Pavements at the Landing Research Runway, NASA Wallops Station. Pavement Grooving and Traction Studies, NASA SP-5073, 1969. (Paper No. 3 herein.)

3. Horne, Walter B.; and Tanner, John A.: Joint NASA-British Ministry of Technology Skid Correlation Study – Results From American Vehicles. Pavement Grooving and Traction Studies, NASA SP-5073, 1969. (Paper No. 23 herein.)

4. Smiley, Robert F.; and Horne, Walter B.: Mechanical Properties of Pneumatic Tires With Special Reference to Modern Aircraft Tires. NASA TR R-64, 1960.

5. Kummer, H. W.; and Meyer, W. E.: Tentative Skid-Resistance Requirements for Main Rural Highways. Rep. 37, Nat. Cooperative Highway Res. Program, Nat. Res. Counc., 1967.

TABLE I.- SITE I (LANDING RESEARCH RUNWAY) TEST SURFACES

Surface	Material	Description
A	Ungrooved concrete	Surfaces A and B were subjected to a canvas belt drag treatment. The goal was to obtain as smooth a surface texture as practically possible. Later, 1- × 1/4- × 1/4-inch transverse grooves were cut in surface B by diamond saws.
B	Grooved concrete	
C	Grooved concrete	Surfaces C and D were subjected to a longitudinal burlap drag treatment. The goal was to obtain a typical currently used runway surface texture. Later, 1- × 1/4- × 1/4-inch transverse grooves were cut in surface C by diamond saws.
D	Ungrooved concrete	
E	Asphalt	The wearing course of surface E was paved with Gripstop, a refined product of Kentucky rock asphalt. The resulting course had a very smooth surface with fine but sharp sand particles exposed.
F	Ungrooved asphalt	Surfaces F and G were paved with asphalt containing 3/8 inch or less aggregate. Later, 1- × 1/4- × 1/4-inch transverse grooves were cut in surface G by diamond saws.
G	Grooved asphalt	
H	Grooved asphalt	Surfaces H and I were paved with asphalt containing 3/4 inch or less aggregate. Later, 1- × 1/4- × 1/4-inch transverse grooves were cut in surface H by diamond saws.
I	Ungrooved asphalt	
A-1	Ungrooved epoxy	Outside lanes of surfaces A and B were given a spray coating of epoxy-grit. (See table II, surface G.)
B-1	Grooved epoxy	

TABLE II.- SITE II (LANDING RESEARCH RUNWAY TAXIWAY) SURFACES

Surface	Treatment	Description
A	Ungrooved	Original concrete taxiway surface with smooth sandy texture. 26-year-old surface
A-1	3/4- × 1/8- × 1/8-inch transverse grooves	
A-2	3/4- × 1/8- × 1/8-inch longitudinal grooves	
B	Ungrooved	Asphalt seal coat overlaying original concrete taxiway surface. 13-year-old surface
B-1	3/4- × 1/8- × 1/8-inch transverse grooves	
B-2	3/4- × 1/8- × 1/8-inch longitudinal grooves	
B-3	1- × 1/8- × 1/8-inch transverse grooves	
B-4	1- × 1/8- × 1/8-inch longitudinal grooves	
D	Asphalt overlay	Local sand mix asphalt, 8% asphalt. New surface
C	Asphalt surface dressing	Asphalt with exposed large aggregate projecting above surface. 13-year-old surface
E	Sinopal asphalt overlay	Plant mix asphalt with 50% aggregate containing Sinopal, a synthetic stone, 25% crushed granite, and 25% silica sand. New surface (furnished by Martin Marietta Corp.)
F	Rolled epoxy coating	Flint abrasive and carborundum with aggregate size of 20-70. Epoxy film thickness was 0.015 to 0.050 inch. Coverage was 40 square feet per gallon using 39.7 grams of aggregate. New surface (furnished by American Abrasive Metals Co.)
G	Sprayed epoxy-grit coating	Grit used was blast furnace slag with average aggregate size of 3/32 inch. Epoxy film thickness was 0.030 inch. New surface (furnished by Devoe & Reynolds Co., Inc.)

TABLE III.- SITE III (SKID PAD) TEST SURFACES

Surface	Treatment	Description
A	3/4- × 1/8- × 1/8-inch transverse grooves on straightaway	The entire concrete surface of the 88- × 450-foot skid pad was covered with liquid Jennite which is a coal-tar emulsion. The usual sand and aggregate content normally used in highway application was omitted in the treatment of the skid pad to obtain as smooth and slippery a skid surface as possible.
B	3/4- × 1/8- × 1/8-inch longitudinal grooves on straightaway	
C	3/4- × 1/8- × 1/8-inch longitudinal grooves on 500-foot-radius-curve lane	
D	Ungrooved 500-foot-radius-curve lane	
E	Ungrooved straightaway	
G	Ungrooved 500-foot-radius-curve lane	

TABLE IV.- AUTOMOBILE STOPPING DISTANCE ON ICE-COVERED SITE I SURFACES AT A GROUND SPEED OF 50 MILES PER HOUR

	Stopping distance, ft	Average friction coefficient
Surface C (1- × 1/4- × 1/4-inch transverse grooved concrete)	146	0.570
Surface D (Ungrooved concrete)	281	0.296

Test conditions: Ice formed on pavement surfaces during flooding operations prior to testing F-4D aircraft. Ambient air temperature was 31° F. Test car was new and equipped with original equipment tires (2000 miles indicated on vehicle odometer). Brakes were applied firmly by driver, locking all four vehicle wheels at entrance onto test surface at speed of 50 mph. Distance to complete stop was measured.

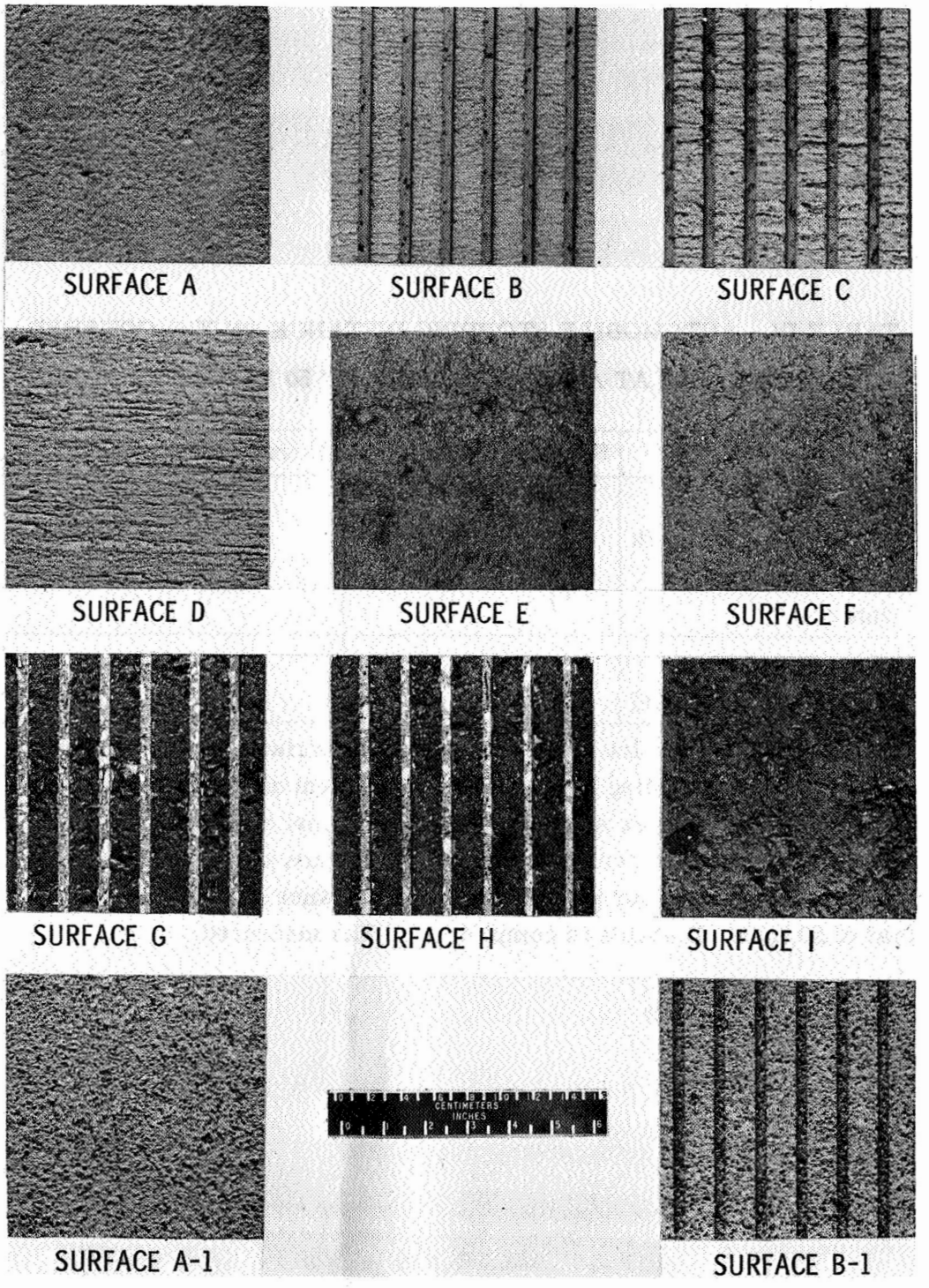

Figure 1.- Test surfaces installed on site 1 (landing research runway). (See table I for test surface description.)

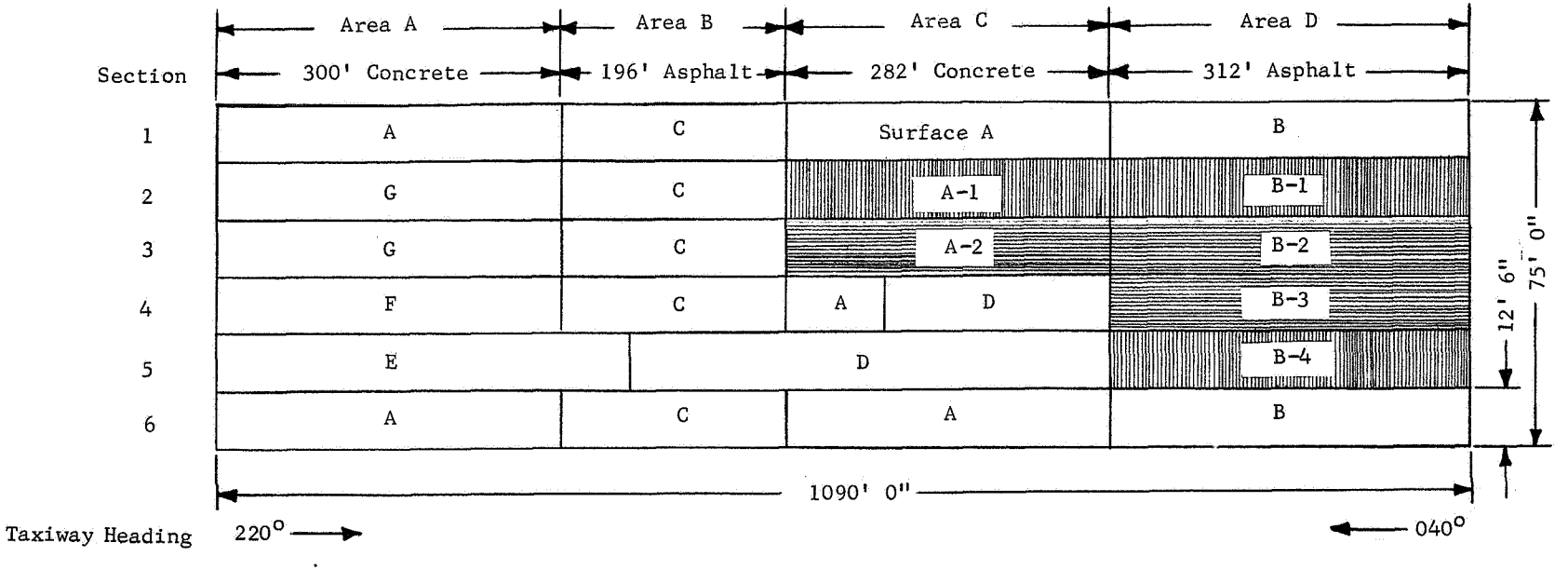

Figure 2.- Layout of test surfaces on site II (taxiway of landing research runway).

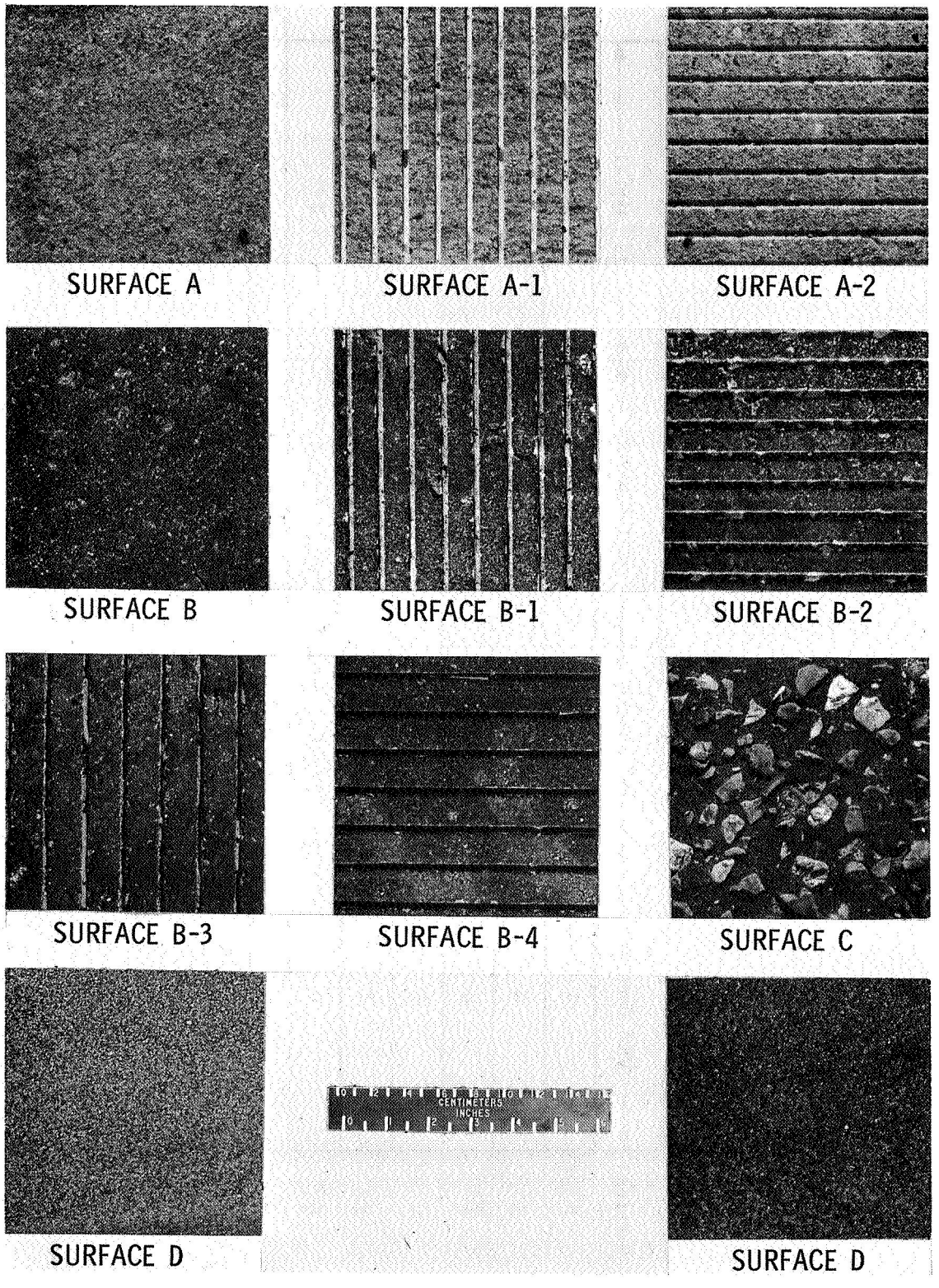

Figure 3.- Test surfaces installed on site 11 (taxiway of landing research runway).

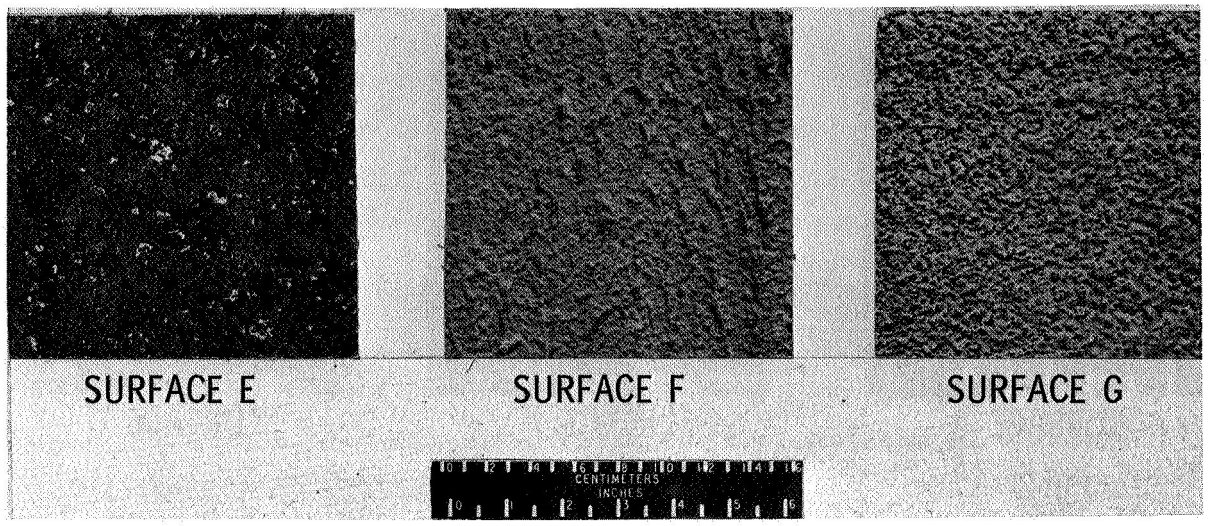

Figure 3.- Concluded.

500-foot radius
Highway curve

Surface
D Ungrooved
G Ungrooved
C Longitudinal grooves; 3/4" x 1/8" x 1/8"

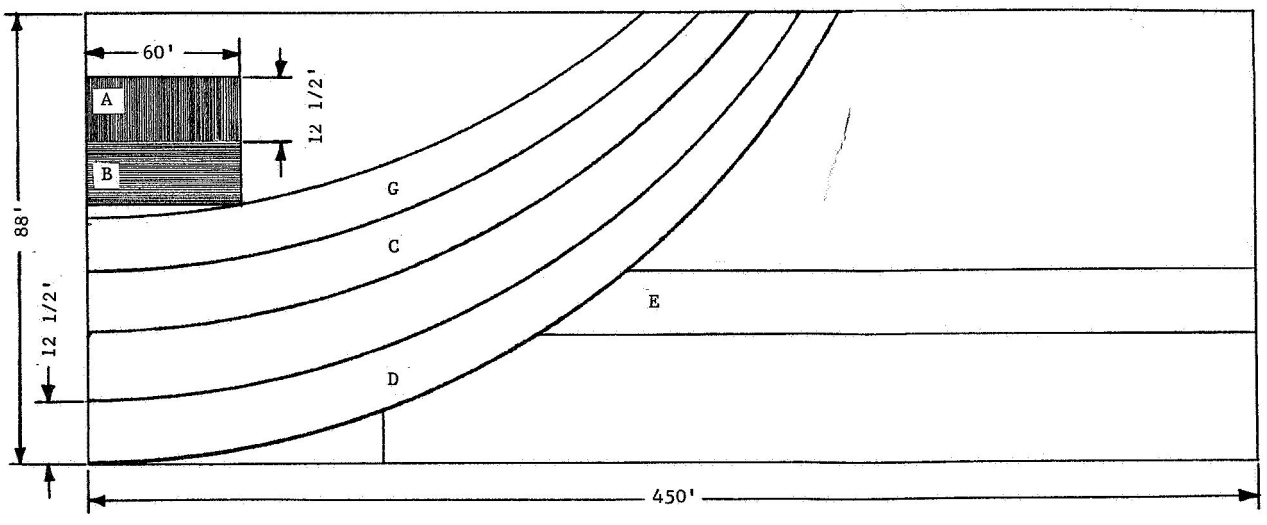

Figure 4.- Layout of test surfaces on site III (skid pad, the hangar apron covered with Jennite, a coal-tar emulsion).

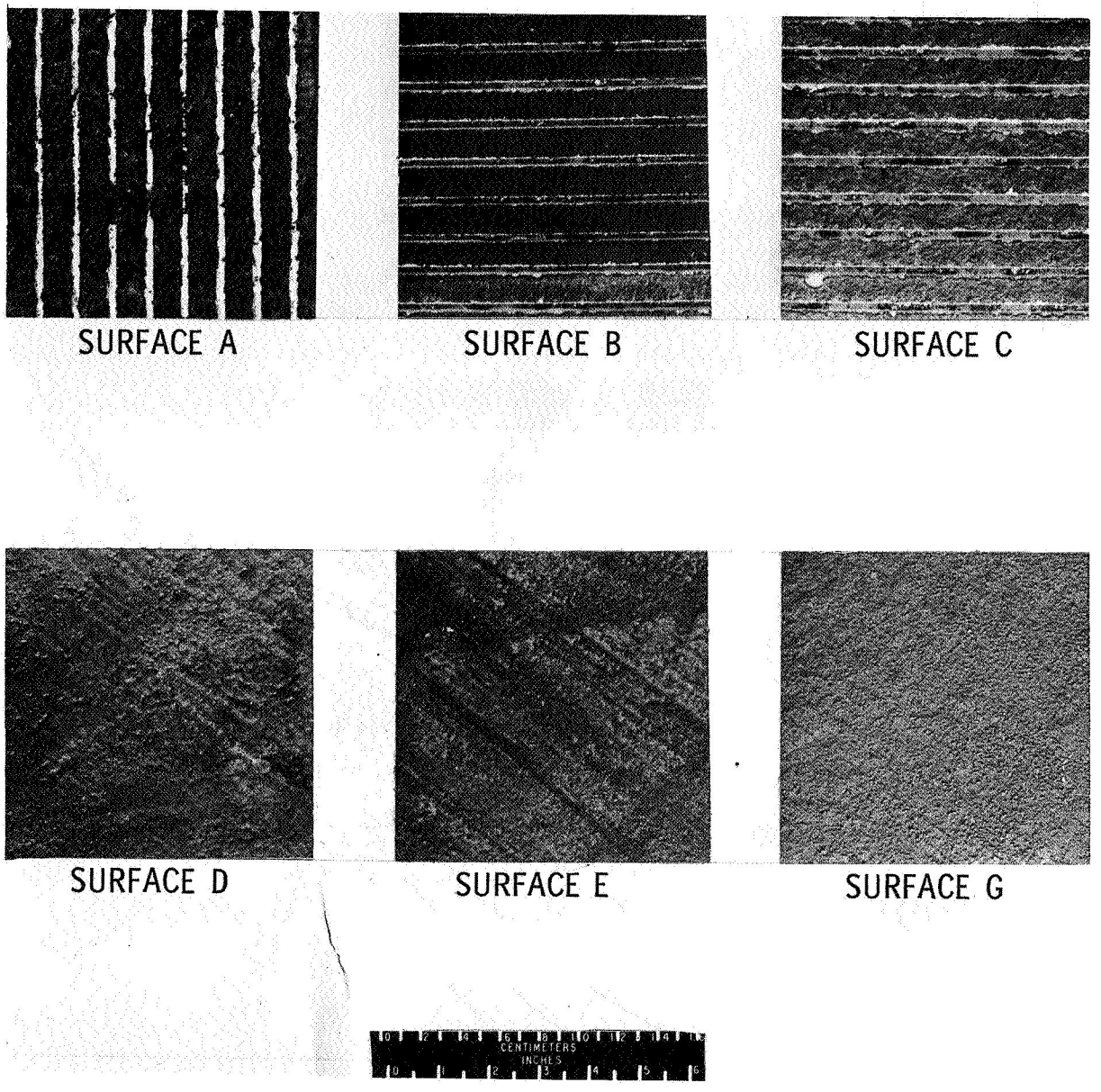

Figure 5.- Test surfaces installed on site III (skid pad). (See table III for test surface description.)

Figure 6.- The British "Juggernaut" test vehicle undergoing a braking test on surface A of site 1 under a wet and puddled pavement condition.

(a) NASA diagonal braking car undergoing test on surface E of site II under a flooded pavement condition provided by plastic-pipe sprinkler system.

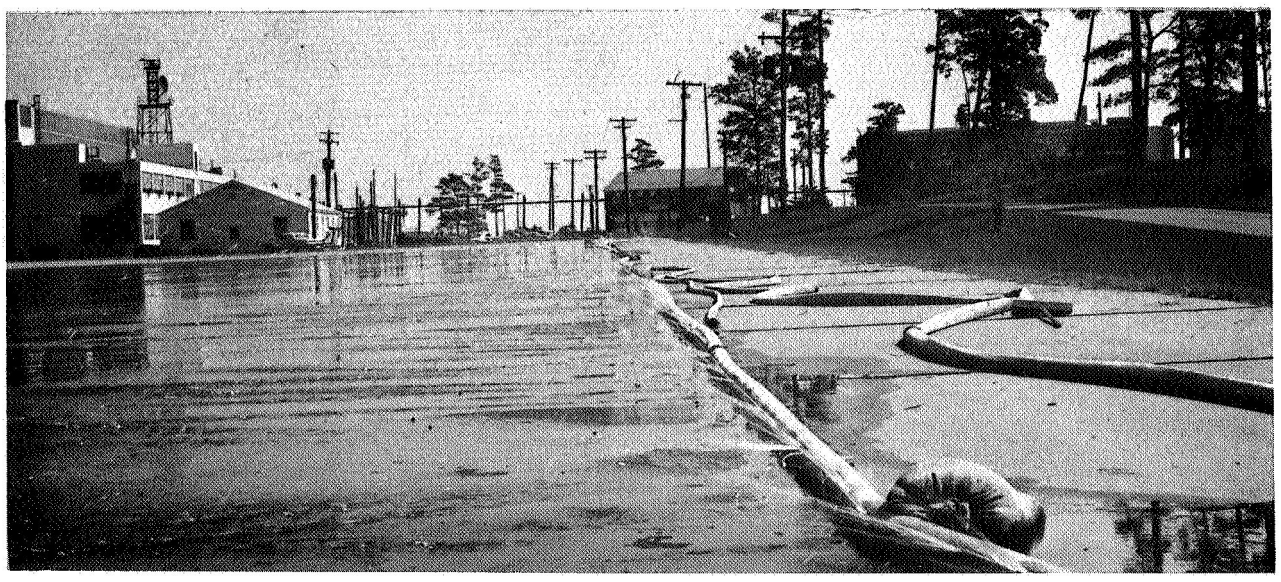

(b) Pierced-canvas-fire-hose sprinkler system used to wet or flood site III skid pad.

Figure 7.- Water sprinkler systems used to wet or flood site II and site III test surfaces.

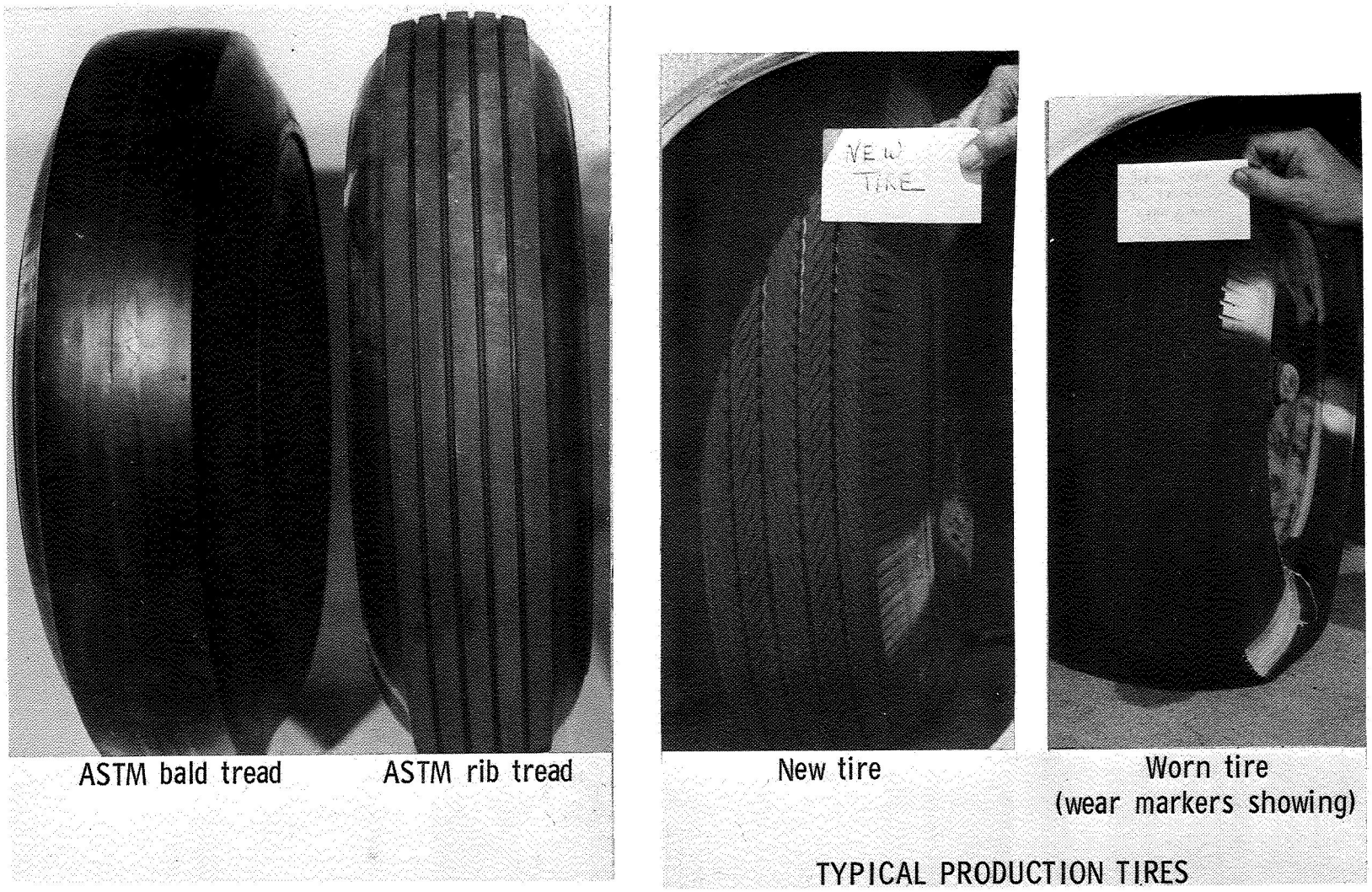

Figure 8.- Tires used on test vehicles to evaluate pavement skid resistance.

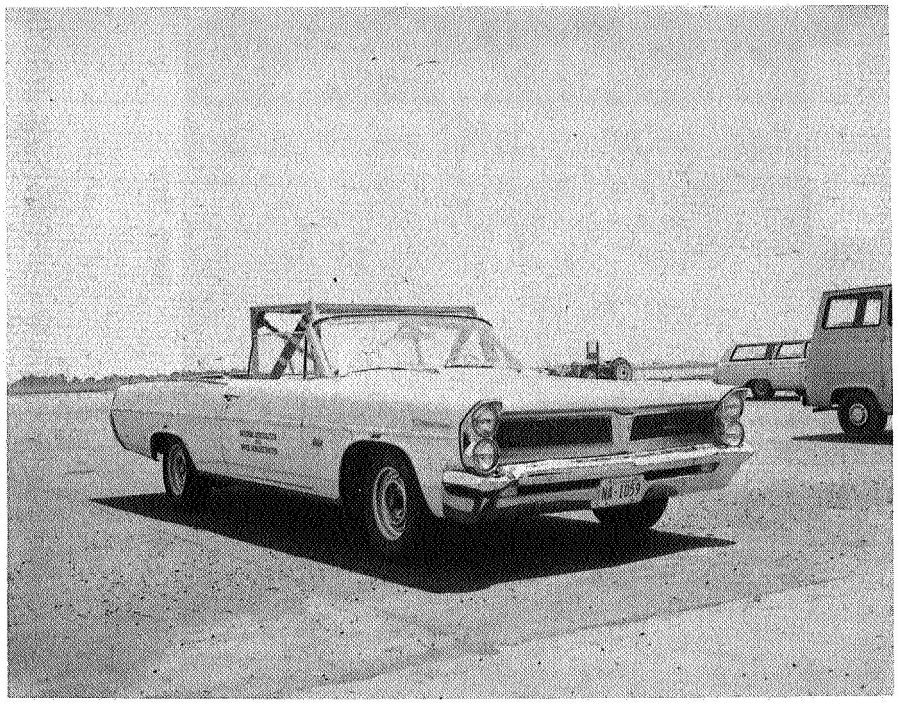

Figure 9.- Stripped convertible with protective cage used by NASA in vehicle spin-out tests on site III skid pad.

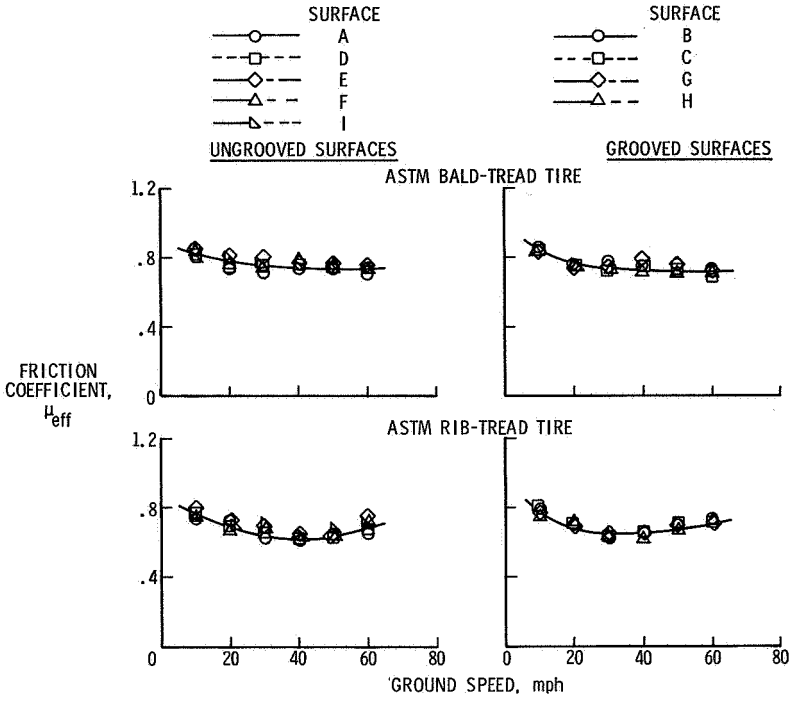

Figure 10.- Skid resistance of site I surfaces rated by NASA diagonal braking car under near transient peak braking conditions. ASTM bald- and rib-tread tires; dry pavement; Tapley meter.

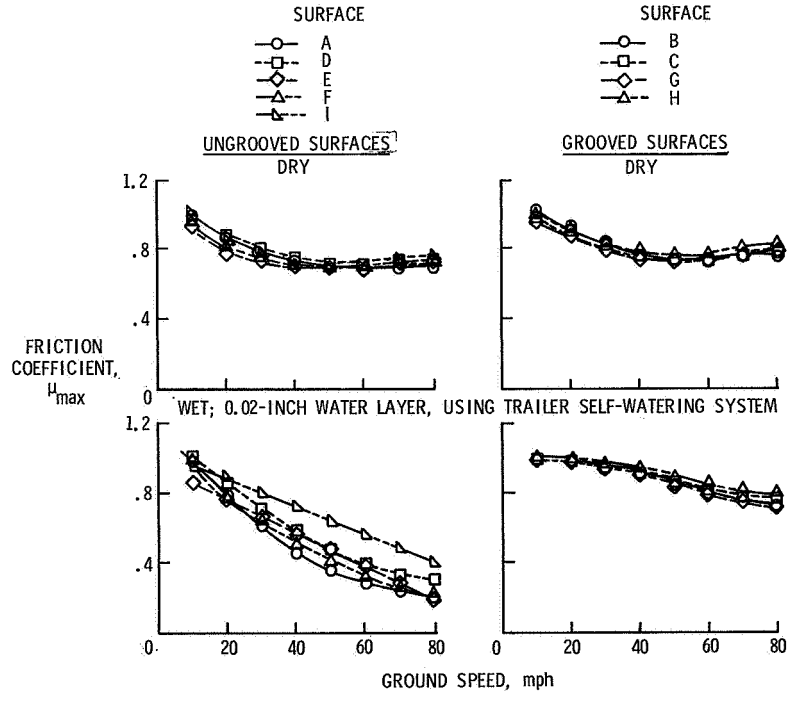

Figure 11.- Skid resistance of site I surfaces rated by FAA Swedish Skiddometer under steady-state peak braking conditions. ASTM bald-tread tire.

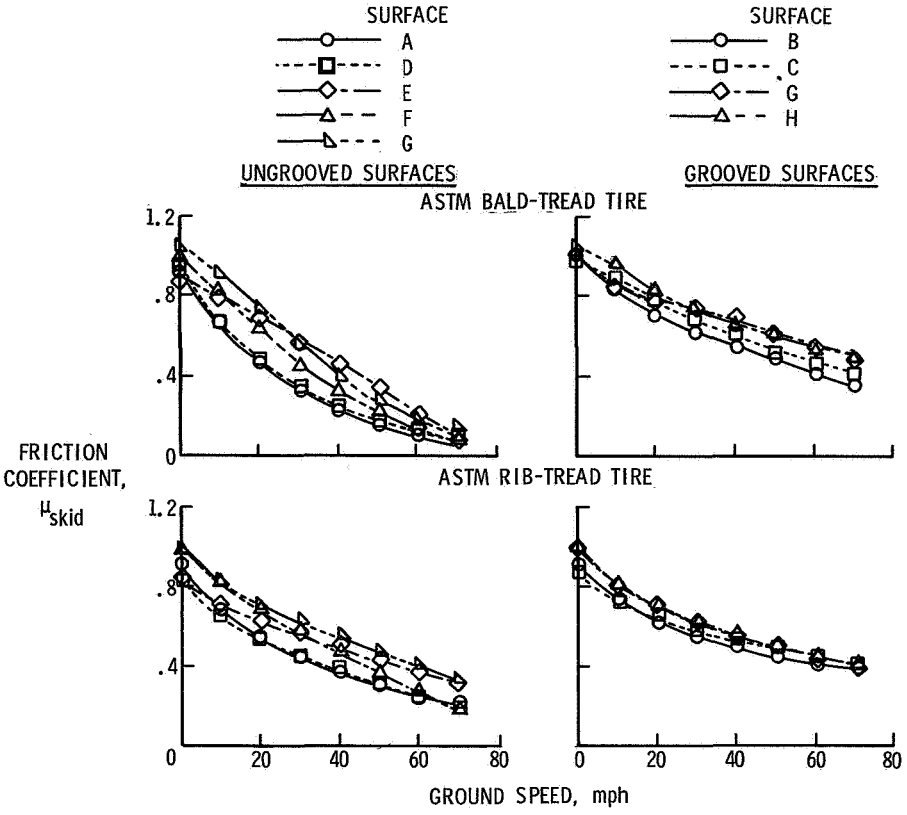

Figure 12.- Skid resistance of site I surfaces rated by NASA diagonal braking car under locked-wheel braking conditions. ASTM bald- and rib-tread tires; wet and puddled surfaces; recording accelerometer.

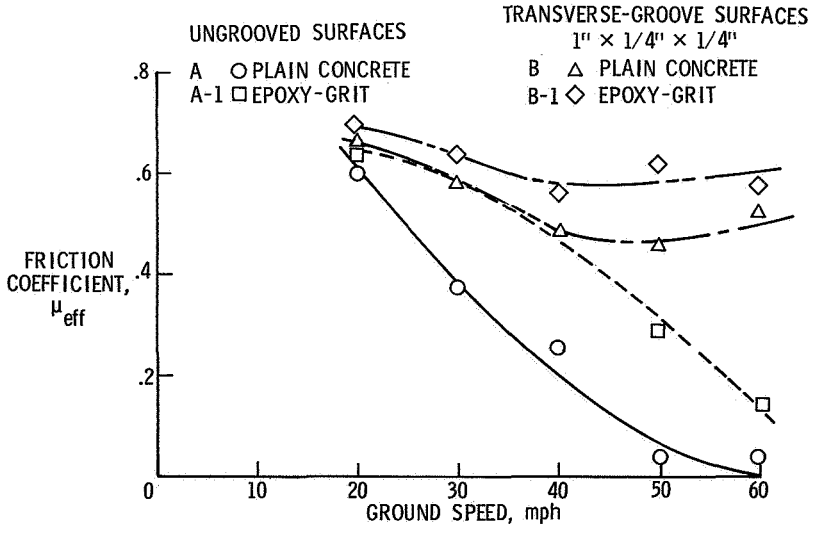

Figure 13.- Improvement in pavement skid resistance by increasing pavement average texture depth by use of epoxy-grit. NASA diagonal braking car; worn tires (wear markers showing); flooded pavement from natural rain; Tapley meter.

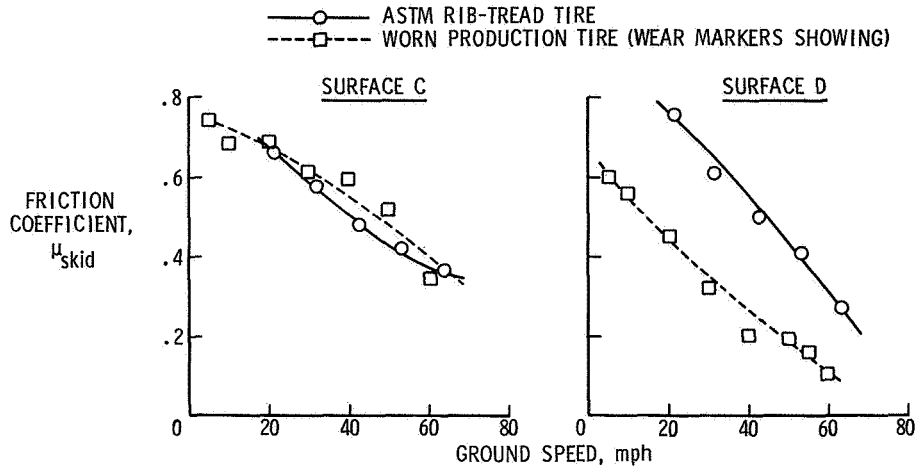

Figure 14.- Comparison of braking performance of ASTM rib-tread and worn production tires on site I surfaces. B. F. Goodrich diagonal braking car; flooded pavement conditions.

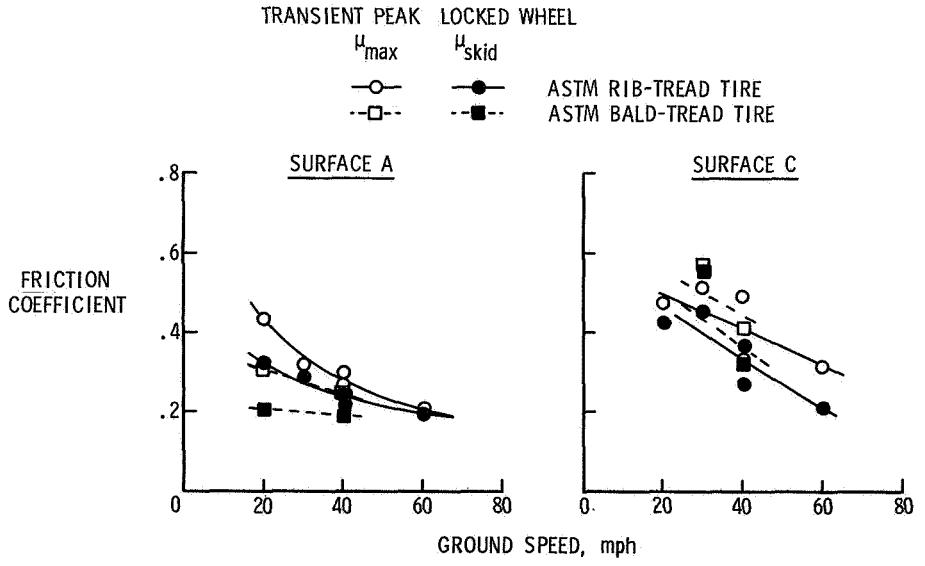

Figure 15.- Skid resistance of site I surfaces under deep slush pavement conditions (0.5 to 2.0 inches). General Motors braking trailer.

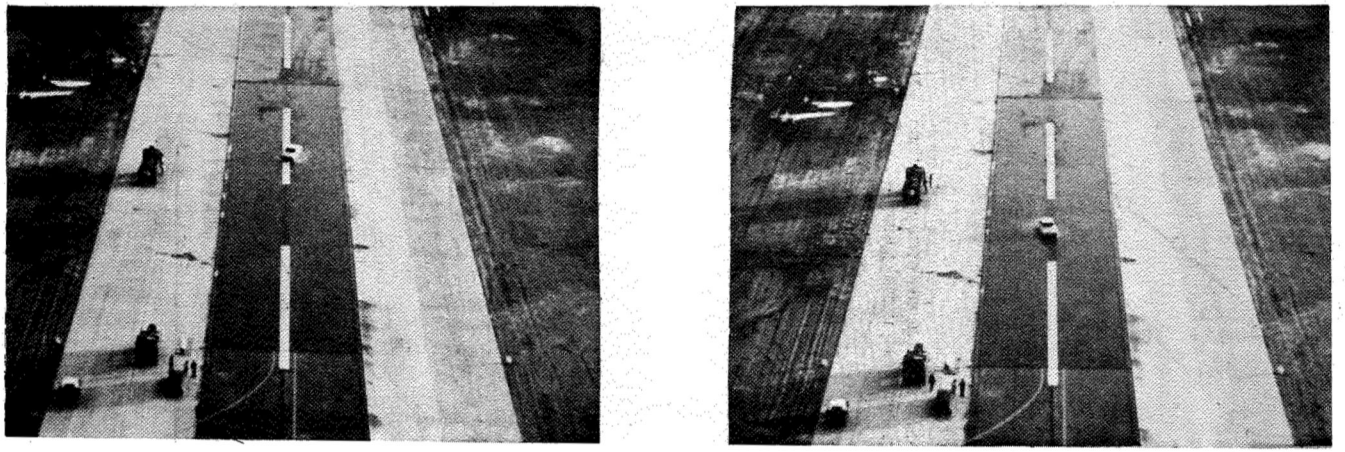

(a) Making "S" turns about runway center line on concrete surface C with 1- × $\frac{1}{4}$- × $\frac{1}{4}$-inch grooves. Vehicle did not skid.

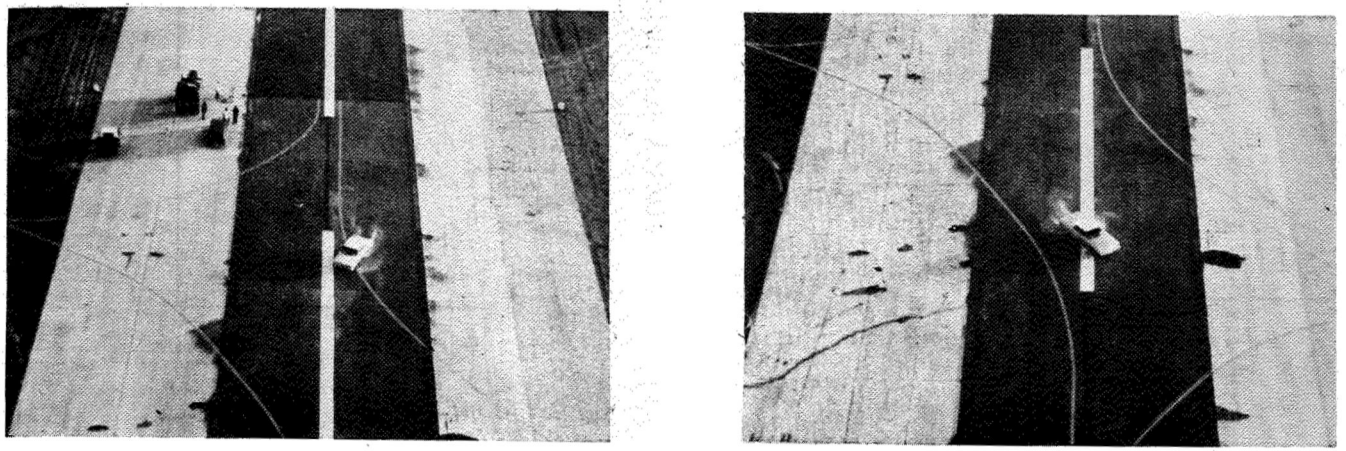

(b) Making "S" turns about runway center line on ungrooved concrete surface D. Same steering input was used as for part (a). Vehicle lost directional control and skidded sideways.

Figure 16.- Vehicle steering and directional control on ice-covered grooved and ungrooved pavements of site I. Vehicle speed, 30 mph; half-worn tires.

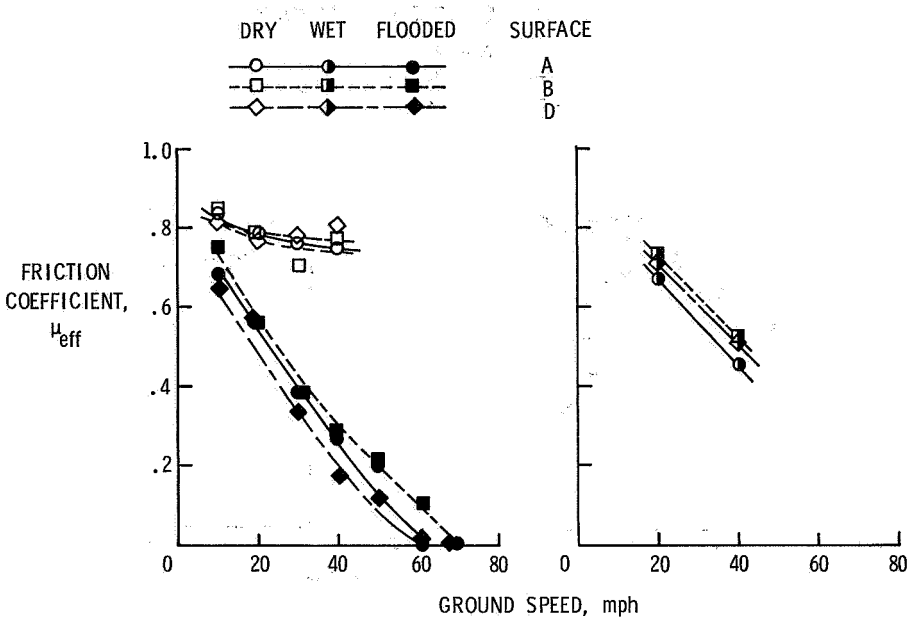

Figure 17.- Skid resistance of conventional site II surfaces. NASA diagonal braking car; Tapley meter; ASTM bald-tread tires.

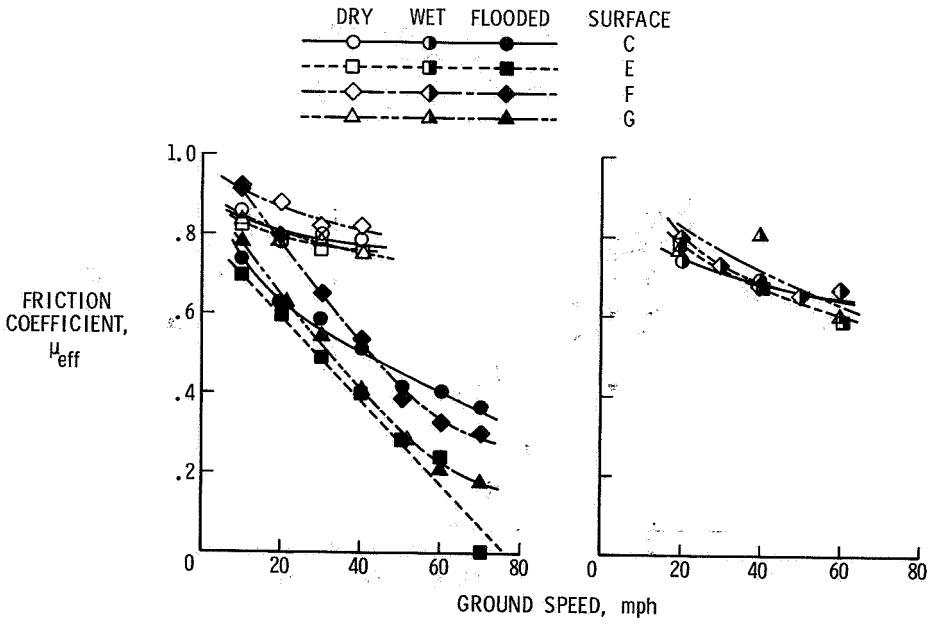

Figure 18.- Skid resistance of treated site II surfaces. NASA diagonal braking car; Tapley meter; ASTM bald-tread tires.

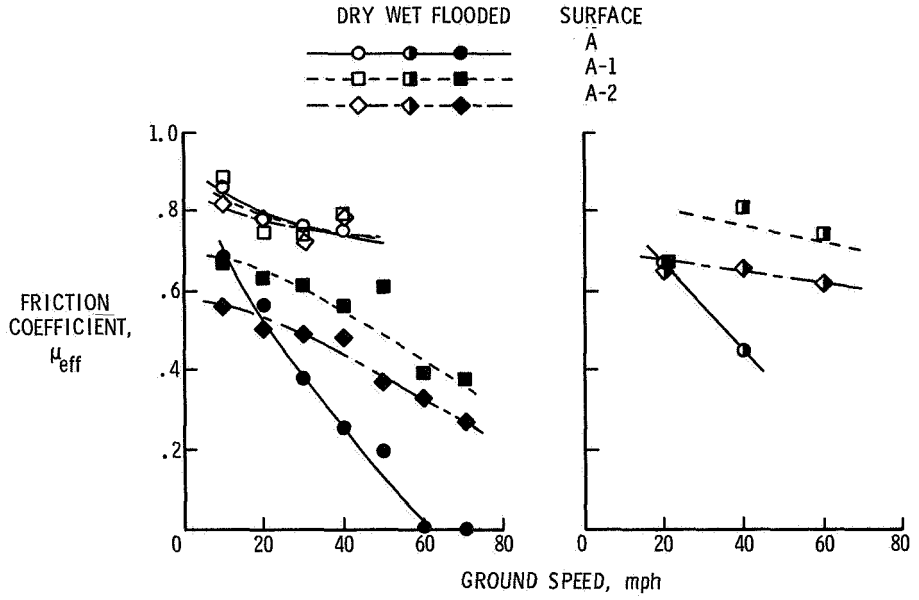

Figure 19.- Improvement in skid resistance of site 11 concrete pavement by using $\frac{3}{4}$- × $\frac{1}{8}$- × $\frac{1}{8}$-inch groove patterns. NASA diagonal braking car; Tapley meter; ASTM bald-tread tires.

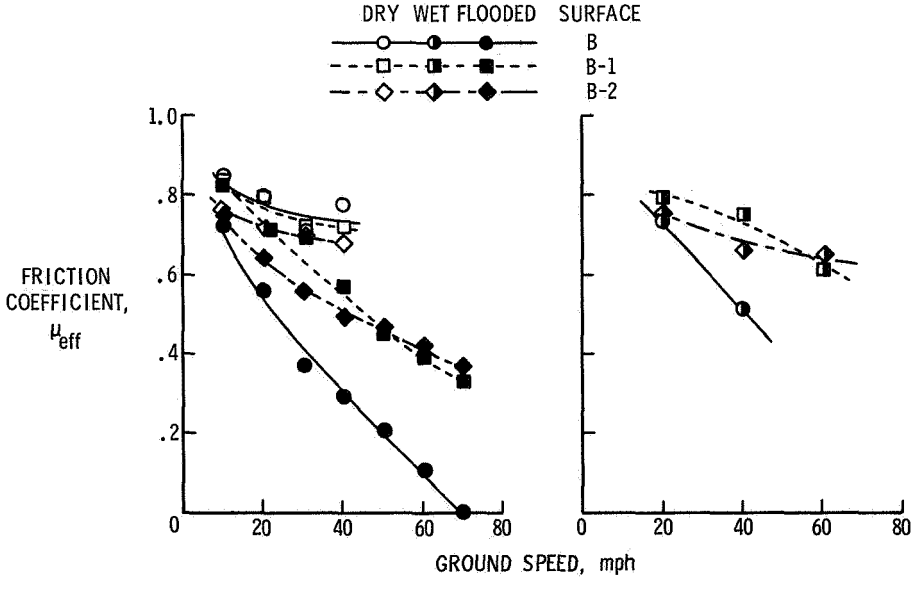

Figure 20.- Improvement in skid resistance of site 11 asphalt (seal coat) pavement by using $\frac{3}{4}$- × $\frac{1}{8}$- × $\frac{1}{8}$-inch groove patterns. NASA diagonal braking car; Tapley meter; ASTM bald-tread tires.

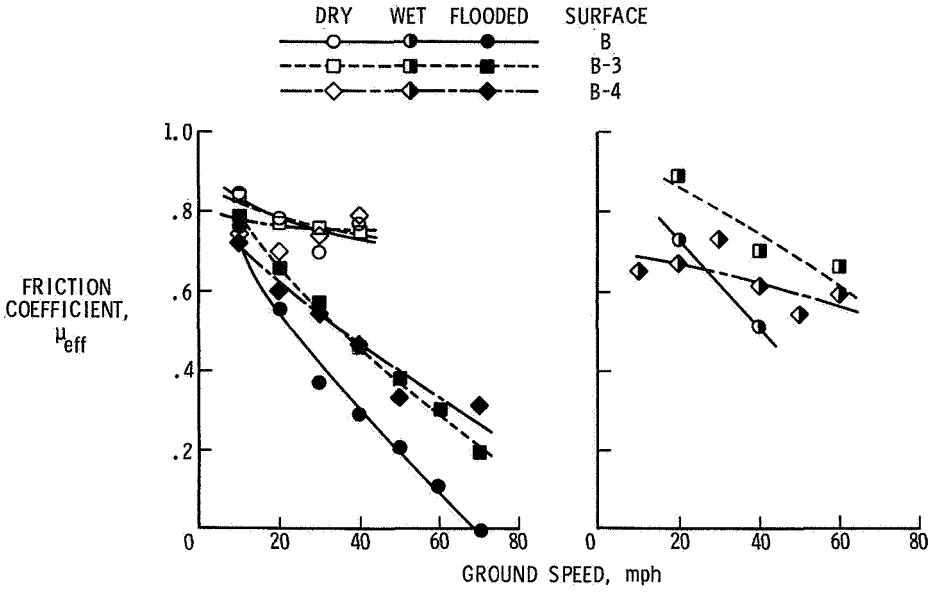

Figure 21.- Improvement in skid resistance of site II asphalt (seal coat) pavement by using 1- × $\frac{1}{8}$- × $\frac{1}{8}$-inch groove patterns. NASA diagonal braking car; Tapley meter; ASTM bald-tread tires.

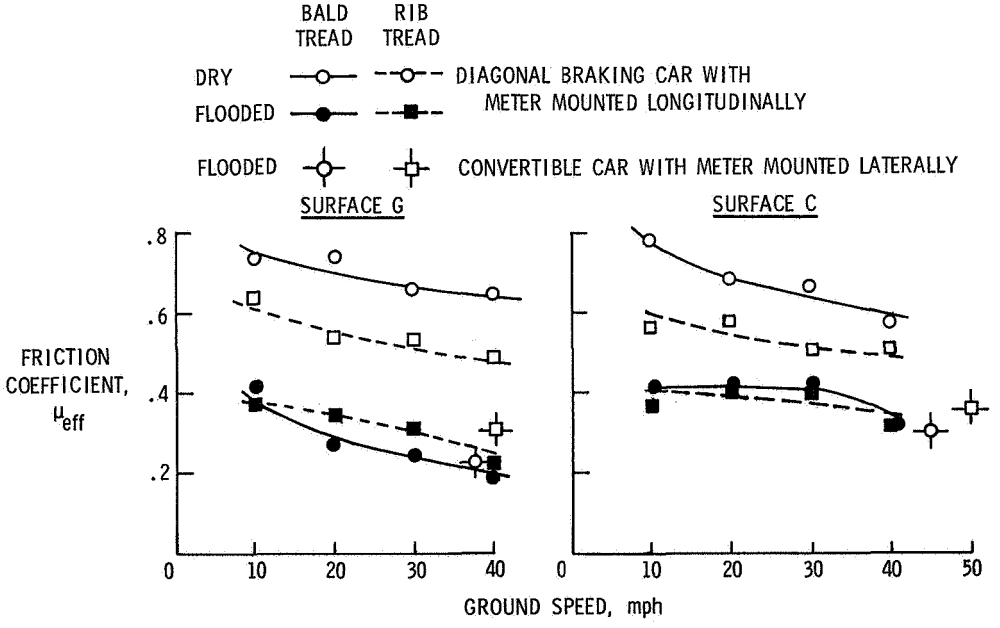

Figure 22.- Comparison of braking and lateral friction coefficients obtained on 500-foot-radius curves of site III skid pad. Jennite surface; NASA diagonal braking and convertible cars; ASTM tires.

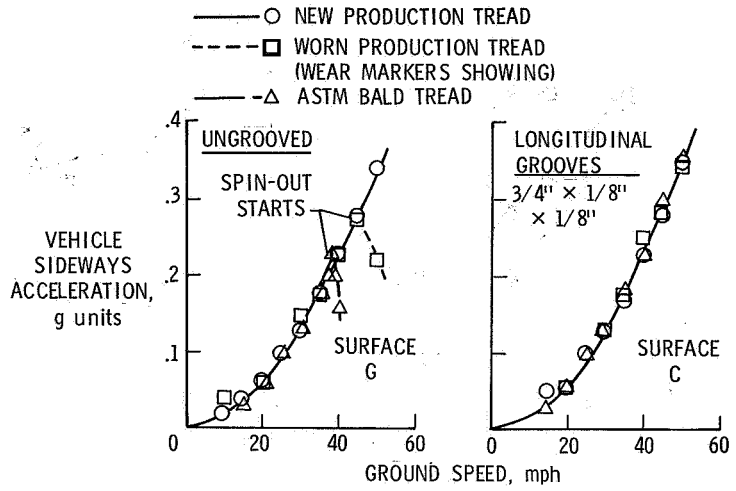

(a) Wet pavement conditions.

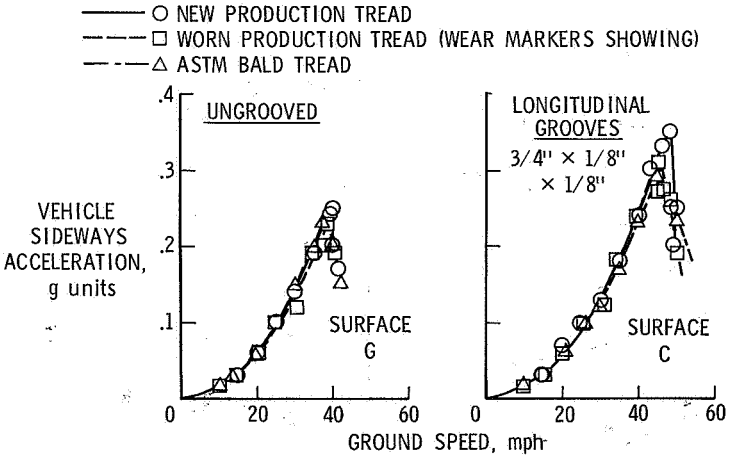

(b) Flooded pavement conditions (0.05 to 0.1 inch).

Figure 23.- Vehicle spin-out speeds obtained on 500-foot-radius curves of site III skid pad. NASA convertible car; Tapley meter mounted sideways.

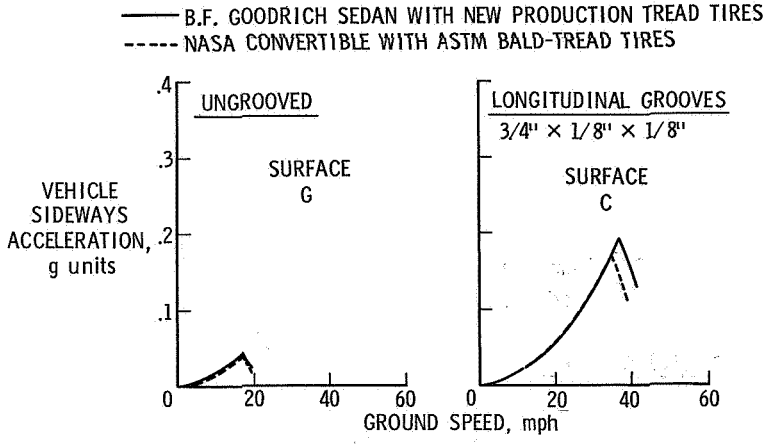

Figure 24.- Vehicle spin-out speeds obtained on 500-foot-radius curves of site III skid pad under slippery pavement conditions (mixture of water and hydrolube).

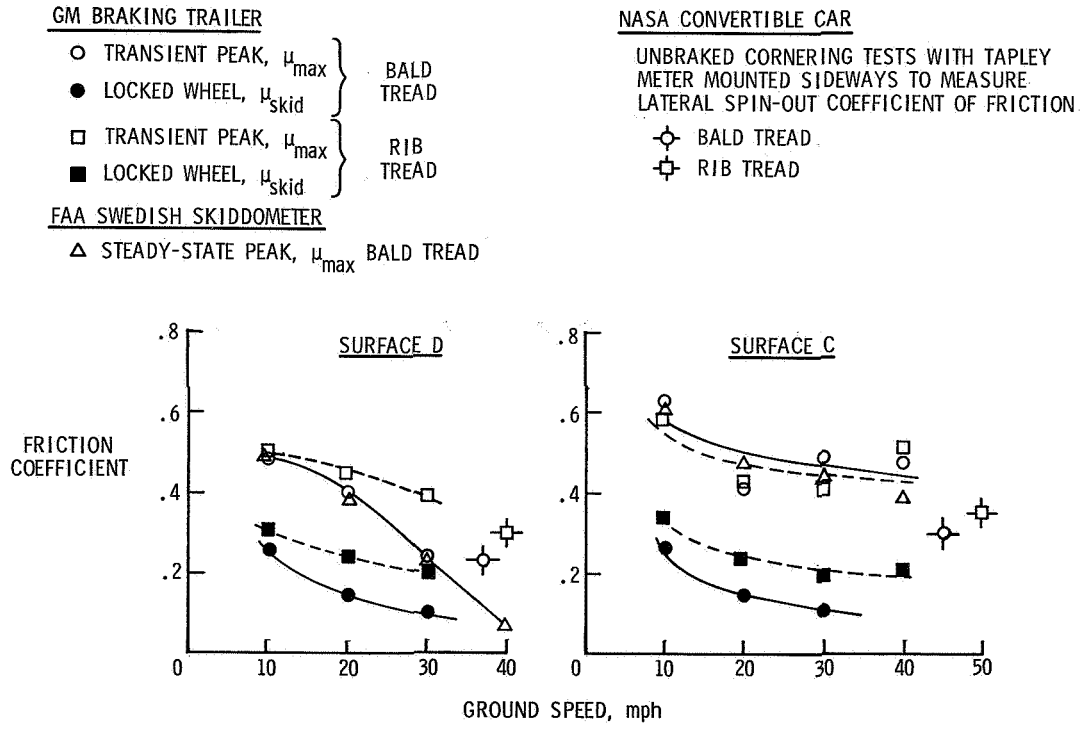

Figure 25.- Comparison of braking and lateral friction coefficients obtained on 500-foot-radius curves of site III skid pad. Flooded pavement conditions; ASTM tires.

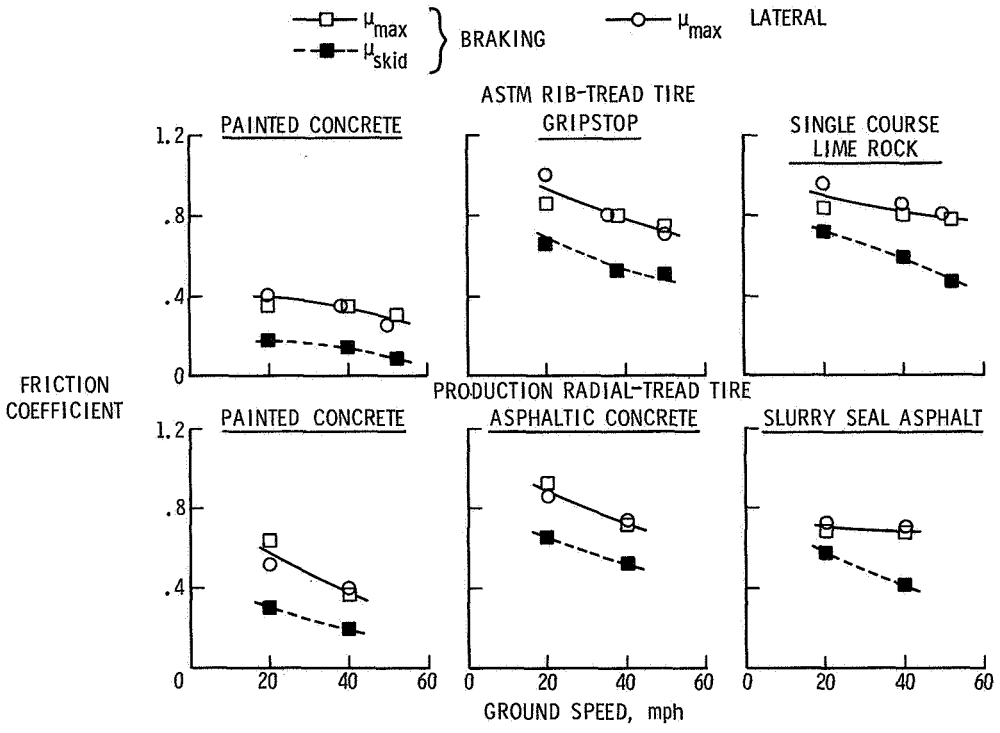

Figure 26.- Comparison of steady-state peak lateral, transient peak, and locked-wheel braking coefficients of friction. NASA research truck; surfaces wetted by sprinkler system; Florida Skid Correlation Study.